Sedimentary Geology 219 (2009) 7–23

Contents lists available at ScienceDirect

Sedimentary Geology

journal homepage: www.elsevier.com/locate/sedgeo

Provenance of the Lower Paleozoic Balcarce Formation (Tandilia System, Buenos Aires Province, Argentina): Implications for paleogeographic reconstructions of SW Gondwana

Udo Zimmermann [a,*], Luis A. Spalletti [b]

[a] Department of Geology, University of Johannesburg, South Africa
[b] Centro de Investigaciones Geológicas (CONICET-Universidad Nacional de La Plata), Calle 1-644, B1900TAC La Plata, Argentina

ARTICLE INFO

Article history:
Received 25 September 2007
Received in revised form 9 February 2009
Accepted 20 February 2009

Keywords:
Provenance
Balcarce Formation
Lower Paleozoic
Heavy mineral study
Argentina

ABSTRACT

Lower Paleozoic moderately sorted quartz–arenites from the Balcarce Formation deposited in eastern Argentina (Tandilia System) comprise mainly detrital material derived from old upper crustal material. The sources were magmatic, sedimentary, and subordinated felsic metamorphic terranes. High concentrations of tourmaline and Ti-rich heavy minerals, including zircon and nearly euhedral chromite, are common. Trace element concentrations (Nb, Cr) on rutile indicate pelitic and metabasaltic sources, respectively. Major element analyses on chromites indicate a basic volcanic protolith of mid-oceanic ridge origin, which was exposed close to the depositional basin. The delivery of chromite may be associated with convergent tectonics causing the consumption and obduction of oceanic crust during pre-Upper Ordovician times. The oblique/orthogonal collision of the Precordillera Terrane with the western border of the Rio de la Plata Craton, west of the Balcarce Basin or source further to the east from a Lower Palaeozoic extensional basin are possibilities.

Geochemical and petrographic data exclude the underlying Precambrian and Cambrian sedimentary rocks as dominant sources, and favour the basement of the Río de La Plata Craton, including Cambrian rift-related granites of South Africa and the Sierras Australes (eastern Argentina), as main suppliers of detritus. Trace element geochemistry of recycled pyroclastic material, associated with the quartz–arenites, also suggests volcanic arc sources. The provenance of the pyroclastic material may either be the Puna–Famatina arc, located in north and central Argentina, or a hypothetical active margin further to the south. These ash layers are equivalent in age to volcanic zircons found in the Devonian Bokkeveld Group in western South Africa.

The deposition of a glacial diamictite of Hirnantian age (Sierra del Volcán Diamictite) is interpreted as a member of the Balcarce Formation. Based on the stratigraphic re-location of the glacial diamictite and trace fossils, the Balcarce Formation is considered here to be Ordovician to Silurian in age. The Balcarce Formation can be correlated with similar rocks in South Africa, the Peninsula Formation, and the upper Table Mountain Group (Windhoek and Nardouw subgroups), including the Hirnantian glacial deposit of the Pakhuis Formation.

1. Introduction

The Balcarce Formation is a Lower Paleozoic succession made of quartz–arenites, kaolinite-rich mudrocks, wackes and conglomerates. These rocks are exposed in the Tandilia System, a northwest–southeast striking mountain belt located 300 km south of Buenos Aires (Fig. 1). In the Tandilia System, Paleoproterozoic crystalline rocks are so far interpreted as the basement (Pankhurst et al., 2003; Rapela et al., 2007). They are covered by Neoproterozoic rocks of the Sierras Bayas Group, which, in turn, are followed by Neoproterozoic–Early Paleozoic mainly fine-grained heterolithic successions known as the Cerro Negro Formation and Punta Mogotes Formation (Fig. 2). The Sierra del Volcán Diamictite, previously assigned to the Neoproterozoic (Iñiguez Rodríguez, 1999), is as young as Ordovician based on detrital zircon age dating (Van Staden et al., 2009) and considered as a member of the Balcarce Formation (Fig. 2).

The Balcarce Formation was unconformably deposited on the basement or the Neoproterozoic sedimentary successions. Based on trace fossils, Poiré et al. (2003) assigned the Balcarce Formation to the Cambrian–Early Ordovician Period. Moreover, parts of the Balcarce Formation might be younger as further trace fossils indicate a Silurian age such as *Cruziana ancora angusta*, *Gyrochorte zigzag* and *Arthrophycus alleghaniensis*, which occur mainly in the eastern part of the basin (Seilacher et al., 2003). SHRIMP analyses on detrital zircon grains allowed Rapela et al. (2007) to report a maximum depositional age of 475–480 Ma.

* Corresponding author. Present address: Department of Petroleum Engineering, University of Stavanger, 4036 Stavanger, Norway. Tel.: +47 51832270; fax: +47 51831750.
E-mail address: udo.zimmermann@uis.no (U. Zimmermann).

0037-0738/$ – see front matter © 2009 Elsevier B.V. All rights reserved.
doi:10.1016/j.sedgeo.2009.02.002

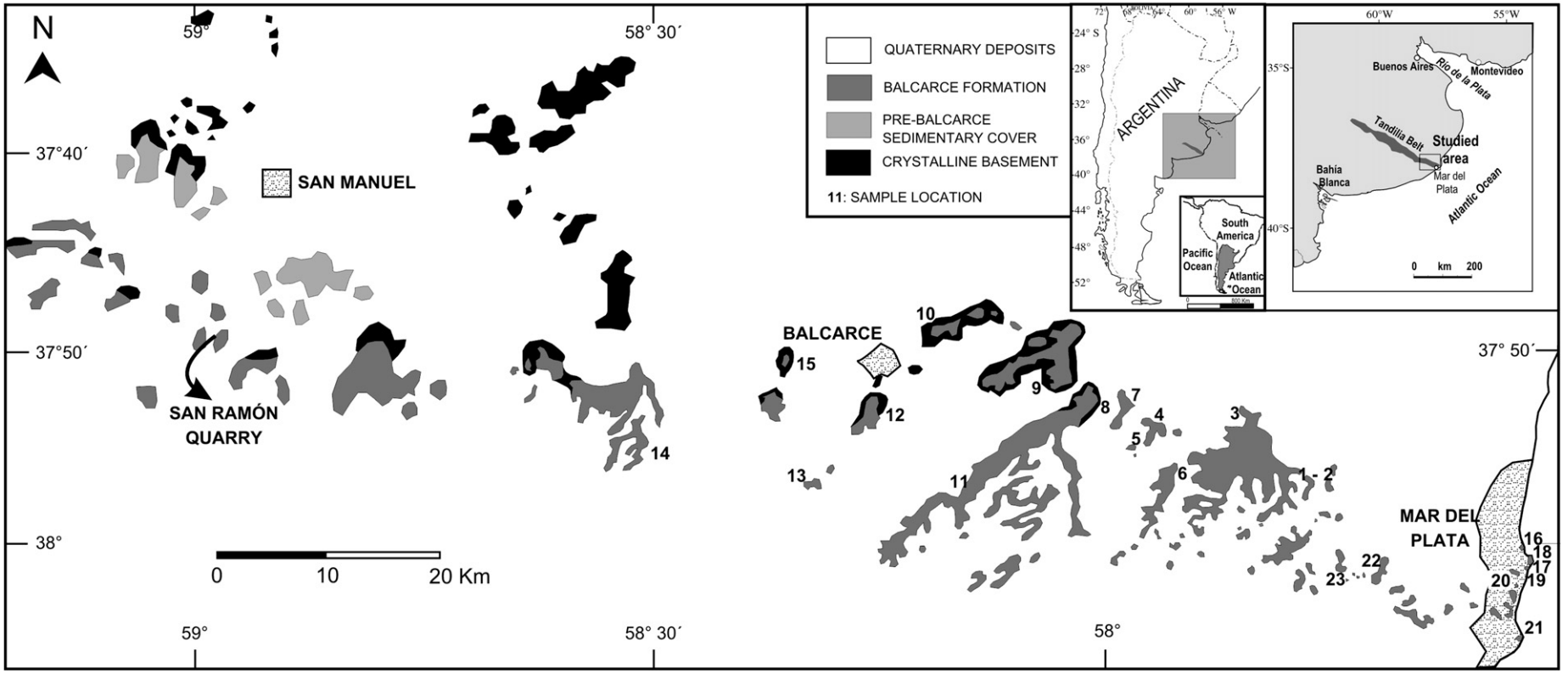

Fig. 1. Location maps and geological map of the eastern sector of the Tandilia System. Sample localities: 1–2: Sierra de Los Padres (simple code SDP), 3: Sierra de Los Difuntos, (SDD), 4: Sierra de Valdés (SDV), 5: Cerro del 10 (SD10), 6: Sierra del 15 (SD15), 7: Sierra La Brava (SLB), 8: Sierra La Vigilancia (SLV), 9: Sierra del Volcán (SEV), 10: Sierra Bachicha (BCH), 11: Sierra La Vigilancia Sur (LVS), 12: Sierra La Barrosa (LBR), 13: Los Pinos (LPN), 14: Sierra Larga Sur (SSL), 15: Cerro Amarante (AMR), 16: Punta Iglesias (PIG), 17: Cabo Corrientes (CCT), 18: Punta Piedras (PPD), 19: Parque San Martín (PSM), 20: Puerto Mar del Plata (PRT), 21: Punta Cantera (PMG), 22: Batán (BTN), and 23: Chapadmalal (CHP).

Eras-Period	*Depositional Sequences*	Stratigraphic Units NW REGION		CENTRAL REGION		SE REGION
SILURIAN						***BALCARCE Formation***
ORDOVICIAN	*Batán Sequence*	***BALCARCE Formation***		***BALCARCE Formation***		Sierra del Volcán Diamictites ***BALCARCE Formation***
CAMBRIAN ?	*La Providencia Sequence*	Cerro Negro Formation		Cerro Negro Formation		Punta Mogotes Formation
(580-590 Ma)	*Villa Fortabat Sequence*	Sierras Bayas Group	Loma Negra Formation	Sierras Bayas Group	Loma Negra Formation	
NEO-	*Diamante Sequence*		Olavarría Formation		Las Aguilas Formation	
PROTERO-	*Malegni Sequence*		Cerro Largo Formation		Cerro Largo Formation	
ZOIC						
(800-900 Ma)	*Tofoletti Sequence*		Villa Mónica Formation		Villa Mónica Formation	
MID-PROTEROZOIC	Crystalline Basement Buenos Aires Complex					

Fig. 2. Modified stratigraphic table of the Tandilia System after Van Staden et al. (in review) based on Poiré et al. (2003).

The siliciclastic deposits of the Balcarce Formation were developed in a nearshore and inner shelf environment on a tide dominated platform, affected by storm events and the marine system was open to the south based on the pattern of progradational clinoforms (Poiré et al., 2003). Paleocurrents indicate a dominant sediment supply from the north for the western and central areas of the Balcarce Formation, where in the eastern part of the basin the main transport directions are eastwest oriented (Teruggi, 1964). The arenites are associated with kaolinite-rich mudrocks, deposits in fine or massive beds (up to 1.5 m). The mudrocks are mostly structureless, but show faint sedimentary structures in the light microscope, like small-scale cross lamination and small channels, defined by slight variations in grain sizes and indicate reworking.

The objective of this paper is to describe the composition of the quartz-rich sandstones of the Balcarce Formation and fine-grained interlayered sedimentary rocks. The wide extension of the Balcarce Formation in the Tandilia System makes this formation one of the key units to understand basin evolution in eastern Argentina during the Lower Paleozoic. The study is based on petrographic analyses by light microscope and SEM, XRD analyses, heavy mineral determination, and electron microprobe analysis of tourmaline, amphibole, rutile and chromite grains as well as whole-rock geochemistry. These studies provide an excellent opportunity to test the potentiality of very mature sandstones and associated rocks in defining the provenance of detrital components, and the paleogeographic and paleotectonic position of a sedimentary basin. These data allow for a correlation between the Argentinean deposits and similar deposits in South Africa (Table Mountain Group).

2. Petrography

The petrographic characteristics of the different lithotypes are in detail compiled in Table 1. The dominating group of rock types is moderate to poorly sorted quartz-rich (up to 98% quartz content) sandstone (Fig. 3a), which occurs in different grain sizes from fine- to coarse-grained, up to conglomerates. Cathodoluminescence (CL) and back-scattered electron microscope (BSE) studies showed that only few quartz grains are well-rounded, as most of them are angular to sub-angular with quartz rims. There is no systematic correlation between grain size and roundness. Feldspar is very rare and mostly only identified by X-ray diffraction technique (XRD) as are kaolinite, illite, glauconite and white mica (Table 2). Sedimentary and metamorphic lithoclasts occur sporadically as do heavy minerals like tourmaline), rutile and zircon.

The second group is made of fine- to coarse-grained wackes enriched in tourmaline and Ti-rich heavy minerals, mainly rutile, but also small amounts of amphiboles, apatite, chromite and zircon. Besides quartz, the rocks are rich in mica, especially in the eastern sector of the basin. Remarkable is the occurrence of kaolinite flakes with the typical morphology of glassy fragments, others display pseudomorphosis after feldspar and replace it (Fig. 3b). Dark brown elongated and wavy formed grains of illite (10 to 35 μm) occur as a rock fragment of probable volcanic origin.

The third group is a unique mudrock composed of quartz, kaolinitisised feldspar and detrital kaolinite. Thick beds typically appear in the San Ramón Quarry (Fig. 1). Quartz grains are mainly angular and most of them show resorption embayments caused by rapid cooling in a volcanic environment (tested after Schneider, 1993 with BSE and CL). Kaolinite clay minerals are flaky, while others appears to be the product of replacement of volcanic glass, as grains are formed like “fiamme” components, welded pyroclastic fragments lying parallel to bedding surfaces. The process of kaolinitisation is beyond the scope of this paper and was studied elsewhere (e.g. Dristas and Frisicale, 1987, 1996). We interpret these rocks based on their texture and sedimentary structures as reworked pyroclastic deposits, either transported primary by wind and then reworked in the Balcarce basin or related to nearer volcanic centres.

3. X-ray diffraction (XRD)

The results of XRD analyses are shown in Table 2. Quartz–arenites of the western area comprise kaolinite and more discrete chlorite and

Table 1
Petrographic and textural characteristics of the main three lihtotypes of the Balcarce Formation here studied.

Quartz-arenites	
General	Poor to moderately or bimodal sorting; grading, cross-bedding
Quartz	Not undulose (20%), pressure solution; angular to sub-angular, rarely well-rounded
Feldspar	K-feldspar, plagioclase (rare, XRD, EDS)
Lithoclasts	Metamorphic (fine sand size, sub-angular, sub-rounded; gneiss, granulite, schist, polycrystalline quartz), Sedimentary (coarse arenites, sub-rounded to sub-angular)
Accessory	White mica, glauconite, tourmaline (80 to 300 μm), rutile (<100 μm), zircon (30 to 280 μm)
Matrix	<3% rarely up to 10%; quartz, muscovite (EDS)
Cement	Quartz overgrowth, patchy microquartz, kaolinite, illite
Fine- and coarse-grained quartz–mica wackes	
General	Poor to moderately or bimodal sorting, grading, cross-bedding
Quartz	Not undulose (30%), pressure solution; angular to sub-angular, rarely well-rounded
Feldspar	K-feldspar, partly entirely kaolinitisised
Lithoclasts	Metamorphic (fine sand size, sub-angular, sub-rounded; gneiss, granulite, schist); sedimentary (siltstone); volcanic (angular kaolinite (glassy fragment-like shape))
Accessory	Muscovite, apatite, zircon, amphibole, chromite
Matrix	10 to 20%; quartz, muscovite, albite (EDS), kaolinite, rutile, illite, amphibole
Cement	Kaolinitic wedges interlayered with muscovite, hydrothermal rutile (EDS, EMPA)
Kaolinite-rich mudrocks	
Texture	Finely laminated, slumps, traction carpets, channels
Quartz	Fine- to medium grained; angular, resorption embayments (volcanic origin; tested by BSE and CL*)
Feldspar	Entirely replaced by kaolinite clay minerals (traces of Na, Ca by EMPA)
Lithoclasts	Flaky fiamme-like fragments entirely replaced by kaolinite clay minerals
Kaolinite	Elongated, flaky and shard-like fragments; replacement of different minerals (unidentified)
Accessory	Titanite
Matrix	80–95%; kaolinite-rich, quartz, hydrothermal rutile(<20 μm)
Cement	–

EDS = energy dispersive spectroscopy; BSE = back-scattered electron microscope; CL = cathodoluminescence; EMPA = electron microprobe analysis; *methodology in Schneider, 1993.

smectite. Those from the central area contain kaolinite, accompanied by muscovite and chlorite. The quartz–arenites of the eastern area are mainly composed of kaolinite with less common illite, chlorite and muscovite. The mudrocks exposed in San Ramón are extremely rich in kaolinite with subordinated illite, chlorite, smectite and muscovite. The wackes from San Ramón are essentially composed of quartz, kaolinite and smectite, while in those from Batán the clay mineral association is kaolinite–illite–muscovite. Rutile is only detectable by XRD in mudrocks and wackes from San Ramón.

4. Heavy mineral studies

Heavy minerals were separated in groups of different grain sizes, but only zircon, chromite and tourmaline showed differences in grain size and form. We could not find any significant difference in heavy mineral composition between the samples of quartz–arenites and wackes. The mudrocks were too fine-grained to be sampled for our purposes. Tourmaline, zircon, chromite, rutile, ilmenite and amphibole are the most abundant (in order of decreasing abundance). Apatite, pyroxene and titanite are accessories.

Titanite is always strongly weathered (50 to 100 μm; Fig. 4a). Apatite grains are subhedral, coarser grained (200 to 350 μm; Fig. 4b) and sometimes include zircon or Th-rich inclusions. Relatively fresh ilmenite (<350 μm) is nearly euhedral (Fig. 4c left), otherwise subhedral (Fig. 4c right) and occurs rarely as smaller grains. Pyroxenes (120–400 μm; Fig. 4d) are mostly broken and strongly weathered, therefore not possible to use for electron microprobe analysis. Amphiboles are subhedral (<120 μm but mostly 250–300 μm; Fig. 4e), relatively fresh but sometimes split along their *c*-axis. Tourmaline (brown to yellow, rarely green) showed nearly any form, but appears mostly broken with well-rounded corners (Fig. 4f left), rarely elongated (Fig. 4f right). Detrital rutile is often subhedral and broken (120–300 μm; Fig. 4g), grains of hydrothermal origin are much smaller (see Fig. 3b). Chromite (150–250 μm; 40–60 μm) is mostly euhedral or corner rounded (Fig. 4h). Seldom, the grains are broken or well-rounded. Of all heavy minerals, zircons display the greatest variety, in size as well as in shape (Fig. 4i), which points to a well mixed provenance (Rapela et al., 2007).

The Balcarce Formation points to a relatively homogeneous heavy mineral composition as the entire basin shows fairly similar occurrences, besides the more rounded grains of tourmaline, which dominate the assemblage in the eastern part of the basin. However, the occurrence of partly euhedral zircon and mostly sub-angular and idiomorphic chromite suggests both, a basic and a felsic source in relative proximity to the depositional area.

5. Whole-rock geochemistry

5.1. Major element geochemistry

Major element geochemistry is a helpful tool when contemplating certain trends in the general composition of rocks, and to decipher the weathering profile of rocks (e.g. Boles and Franks, 1979; Nesbitt and Young, 1982; Nesbitt et al., 1996). However, it is not always applicable for provenance purposes (e.g. Amstrong-Altrin and Verma, 2005) in contrast to trace element geochemistry (e.g. McLennan et al., 1990, 1993).

The quartz–arenites are expectantly extremely enriched in silica (>93 wt.%) and thus depleted in all other major elements. Interestingly, in some samples TiO_2 is more concentrated than alkaline elements (AMR, SEV, SD15; see Table 1 supplemental data). Fe_2O_{3T} is the most abundant major element apart besides Al_2O_3 and silica. The fine- and coarse-grained wackes of San Ramón and Batán nearly show typical upper continental crustal composition (UCC after McLennan et al., 2006)

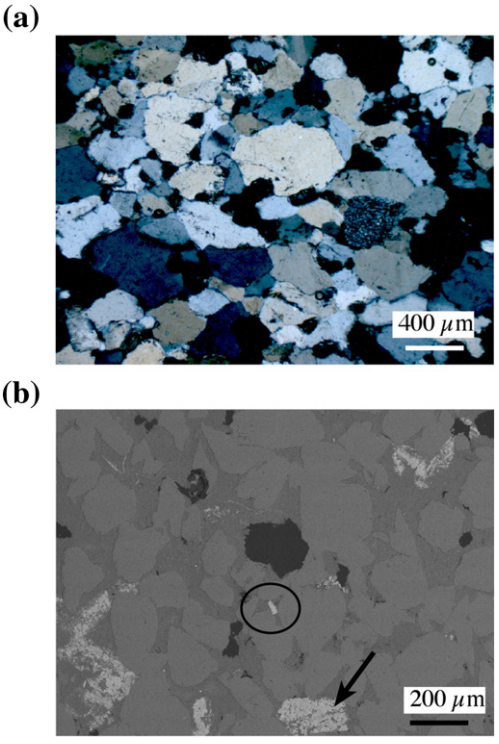

Fig. 3. Images of thin section of the Balcarce Formation. a) Representative sample of the Balcarce Formation (light microscope photograph, polarized light). b) BSE image of a wacke. The circle includes an altered hydrothermal rutile crystal. The arrow points to an example of kaolinite replacement of a feldspar. EDS analyses showed that this crystal comprises still significant amounts of Ca and Na. Magnification (M): 95×.

Table 2
XRD analyses for the samples of the Balcarce Formation.

Area	Locality	Sample	Lithotype	KFS	plg	ill	chl	mus	bt	kao	sme	rut
Western	San Ramón	286	M			x	x			x	x	x
	San Ramón	287	M							x		
	San Ramón	288	M	x						x		x
	San Ramón	290	M							x		x
	San Ramón	291	M	x		x				x		
	San Ramón	292	M	x			x			x		
	San Ramón	293	M	x			x	x	x	x	x	
	San Ramón	296	M			x		x		x		
	San Ramón	296A	M							x	x	x
	San Ramón	294	WA	x						x	x	x
	San Ramón	295	WA							x	x	x
	San Ramón	297	WA			x				x	x	
	Sierra Larga Sur	SSL	QA	x			x					
	Cerro Amarante	AMR	QA	x						x	x	
	Los Pinos	LPN	QA	x			x					
	Sierra La Barrosa	LBR	QA	x						x		
Central	Sierra Bachicha	BCH	QA	x			x			x		
	Sierra La Vigilancia Sur	LVS	QA	x								
	Sierra del Volcán	SEV	QA	x								
	Sierra La Vigilancia	SLV	QA	x								
	Sierra La Brava	SLB	QA				x	x		x	x	
	Cerro del 10	SDIO	QA				x			x		
	Sierra de Valdes	SDV	QA	x				x		x		
	Cerro del 15	SDI5	QA	x			x	x				
	Sierra Los Difuntos	SDD	QA									
Eastern	Sierra de Los Padres	SDP1	QA			x	x					
	Sierra de Los Padres	SDP2	QA	x		x				x		
	Chapadmalal	CHP	QA	x	x			x				
	Batán	BTN	QA	x	x					x	x	
	Batán	270	QA	x		x	x	x		x		
	Batán	272	QA	x		x				x		
	Batán	273	QA	x						x		
	Batán	273A	QA	x						x		
	Batán	275	QA					x		x		
	Batán	277	QA	x						x		
	Batán	278	QA	x		x				x		
	Batán	274	WA			x		x		x		
	Batán	276	WA			x				x		
	Batán	279	WA	x				x		x		
	Punta Cantera	PMG	QA	x			x			x		
	Puerto Mar del Plata	PRT	QA	x			x	x				
	Parque San Martin	PSM	QA	x								
	Cabo Corrientes	CCT	QA	x								
	Punta Piedras	PPD	QA	x								
	Punta Iglesias	PIG	QA	x								

Only abundant phases are detected. Note that quartz is not shown, as it is component in all samples. KFS comprises albite, orthoclase, microcline and sanidine. The samples are geographically from west to east (top to bottom) in the table organized. (KFS = alkali feldspar; plg = plagioclase; ill = illite; chl = chlorite; mus = muscovite; kao = kaolinite; sme = smectite; rut = rutile).

in silica (53 to 76 wt.%). They are enriched in Al_2O_3 (12 to 26 wt.%), caused by the kaolinite-rich matrix, and in TiO_2 (1.3 to 4.6 wt.%) as hydrothermal rutile was introduced. This trend is also observable in the kaolinite-rich mudrocks, with low concentrations in Fe_2O_{3T}, CaO, MgO and Na_2O, but enrichments in TiO_2 and Al_2O_3 (Table 1 supplemental data). In contrast, these samples are depleted in K_2O (mostly <0.3 wt.%) and silica (mainly <50 wt.%).

5.2. Alteration

Alteration of sedimentary rocks can be determined by different means, including the CIA index (Chemical Index of Alteration, after Nesbitt and Young, 1982; Fedo et al., 1995), K/Cs (McLennan et al., 1990) or Th/U ratios (McLennan et al., 1993) that have all been successfully applied in several case studies in the past (e.g. McLennan et al., 1993; Hurowitz and McLennan, 2005; Van Staden et al., 2006).

However, all these approaches are difficult to apply to the Balcarce Formation as the quartz–arenites mostly comprise Al + Na + K + Ca (wt.% oxide) concentration below 2%. Thus, the CIA values do not reflect the weathering profile, as the element concentration taken into account is by far not representative for the rock. The situation is similar when calculating the K/Cs ratio, where Cs is severely depleted. On the other hand, the kaolinite-rich samples are strongly altered with CIA values close to 100%, and Cs concentrations below UCC (after McLennan et al. (2006): 4.6) revealing unreliable K/Cs ratios (Table 1 supplemental data). The relatively high abundance of kaolinite in the matrix of the wackes also causes a high CIA, and two of the five wacke samples have high Cs concentrations, pointing to a strong weathering in accordance to high CIA values (Table 1 supplemental data). Sorting played a significant role on the detrital composition for the quartz–arenites and could have affected the Th/U ratio. However, the quartz–arenites display Th/U ratios over the UCC value, as the wackes do (after McLennan et al. (2006): 3.8; Table 1 supplemental data). Some kaolinite-rich mudrocks show a slight enrichment in Th without a loss of U, but most of the samples display Th/U ratios close to the UCC value (Table 1 supplemental data).

5.3. Trace element composition

An estimation of the composition of sedimentary rocks can be determined using the ratios Zr/Ti versus Nb/Y (after Winchester and Floyd, 1977; Fralick, 2003; Van Staden et al., 2006; Fig. 5a), as these

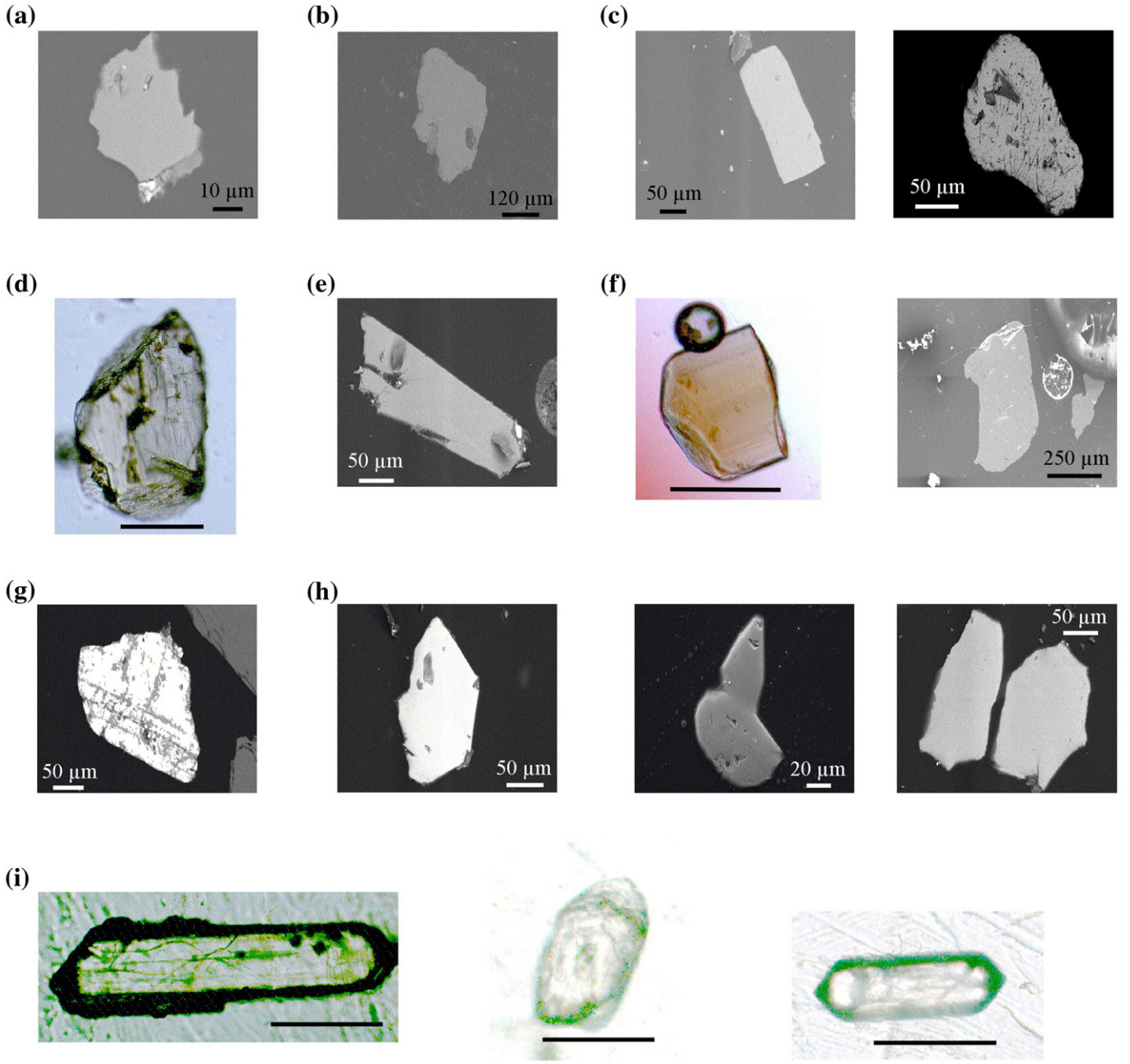

Fig. 4. Images of separated heavy minerals of the Balcarce Formation. a) Titanite grain (BSE image; Magnification (M): 1770×). b) Apatite grain (BSE image; M: 220×).). c) Left: euhedral ilmenite grain (SEM image; M: 270×), right: altered ilmenite grain (BSE image; M: 500×). d) Pyroxene grain (light microscope photograph, polarized light, scale is 100 µm). e) Amphibole grain (SEM image; M: 400×). f) Left: part of a tourmaline grain (light microscope photograph, polarized light, scale is 50 µm), right: tourmaline grain (SEM image; M: 150×). g) Rutile grain (BSE image). h) Several chromite grains, two euhedral (left and centre), one subhedral (centre) and two sub-angular (right) (left: SEM image, M: 450×; centre: SEM image, M: 700×; right: SEM image, M: 400×). i) Zircon grains (light microscope photograph, polarized light; left: scale is 50 µm, centre: scale is 100 µm; right: scale is 50 µm); large elongated zircons with a variety of cracks and inclusions (Fig. 4i left), well-rounded grains (Fig. 4i centre), small prismatic crystals (Fig. 4i right).

elements are strongly immobile. Most of the quartz-rich samples are of a rhyolitic to rhyo-dacitic composition. Some samples from the quarries San Ramón and Batán are partly enriched in Nb over Y and have a lower Zr/Ti ratio than the quartz–arenites. This points to a more alkaline basaltic trend, especially for the mudrocks and might be triggered by the influence of hydrothermal rutile.

General trace element trends can be observed in normalizing the absolute concentrations to UCC (after McLennan et al., 2006; Fig. 5b). The quartz–arenites are nearly depleted in all elements in regard to UCC, but in Cr (in italic letter). However, Cr is difficult to interpret because the samples were milled with a Cr-steel dish and should be discarded (see Sampling and analytical methods). However, the values in Table 1 supplemental data show that some samples comprise high concentration of Cr, which cannot be introduced by milling contamination only. This fact can be corroborated with observations of the heavy mineral fraction, which displayed a high amount of chromite. Zr and Hf concentrations are low and do not reach UCC values although rocks are reworked.

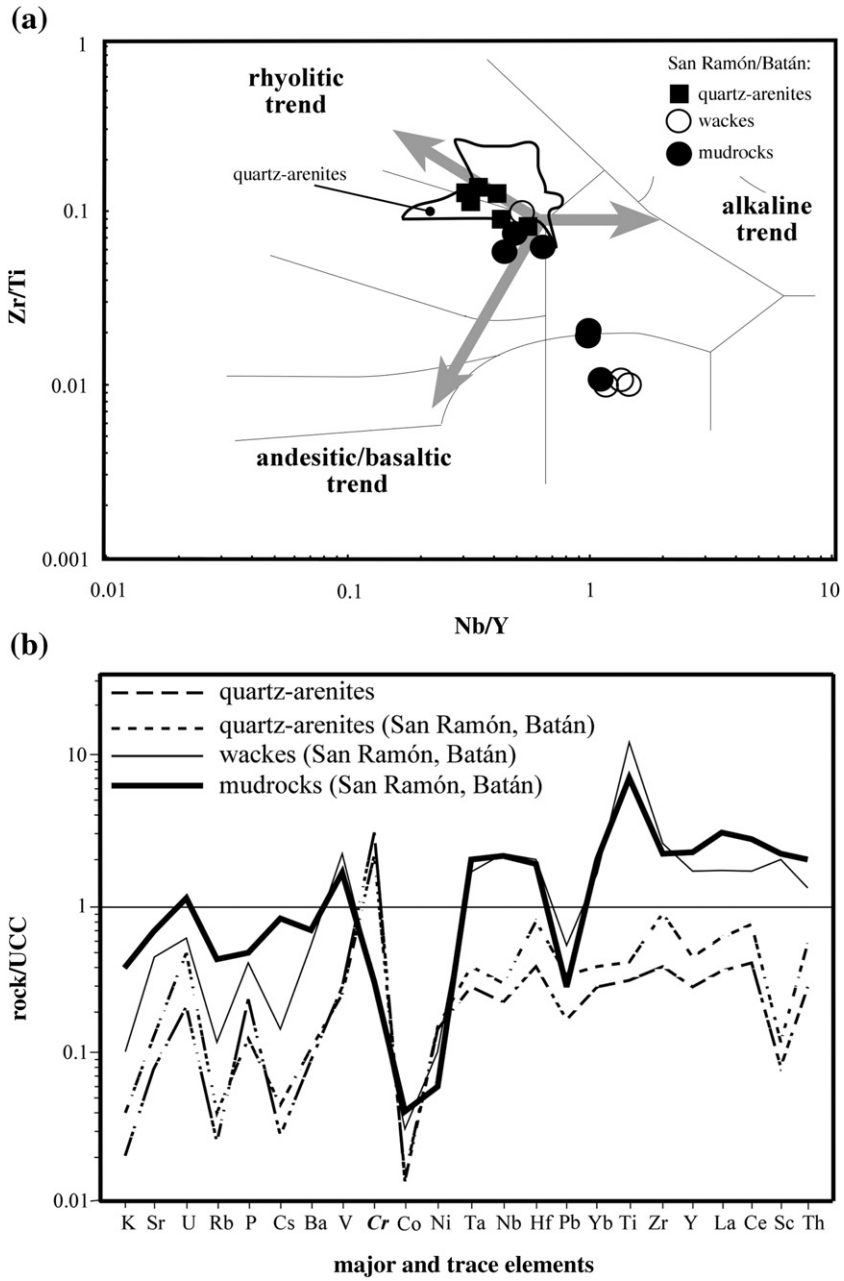

Fig. 5. a) Geochemical diagram to reveal differences in the whole-rock composition of the three groups of the Balcarce Formation (after Winchester and Floyd, 1977). b) Normalization of major and trace elements to upper continental crust averages (after McLennan et al., 2006; diagram after Floyd et al., 1990). Note the relative similarity of the pattern shape for all three groups in LILE but the differences in HFSE. Cr (in italic letters) values are recalculated and should only be interpreted regarding a trend, which demonstrates the scarcity of Cr in the mudrocks in contrast to the quartz–arenites.

Wackes and kaolinite-rich mudrocks show a clear distinct pattern and are enriched in Ta, Nb and Ti. In comparison to the wackes, the kaolinite-rich mudrocks are stronger enriched in most of the large-ion lithophile elements (LILE; K, Sr, Rb, Cs, Ba) and high-field strength elements (HFSE; REE, Th, Zr), but depleted in Pb, Ni and Ti. The enrichment of the compatible element Sc, abundant in mafic minerals like pyroxene and olivine, is important to notice.

5.4. Rare earth elements (REEs)

Quartz–arenites show patterns comparable to PAAS (Post-Achaean Average Australian Shale after Nance and Taylor, 1976) indicating an upper continental crust composition, but they are diluted in REE (Fig. 6). The quartz–arenites from San Ramón and Batán (Fig. 1) comprise three different samples. One is enriched in light REE (LREE) in comparison to PAAS, another one is similar, while a third one (02-292) displays a pattern different to PAAS. The relative enrichment in all REE can be caused by the addition of heavy minerals and the heavy REE (HREE) specifically by zircon, as Zr and Hf concentration in 02-292 are much higher than in all other quartz–arenites (Table 1 supplemental data). The wackes show comparable patterns to PAAS with slightly lower HREE (Fig. 6). The mudrocks are strongly enriched in all REE, which might reflect also heavy mineral addition.

La_N/Yb_N (where "N" expresses chondritic normalization) ratios are relatively high (7.9 to 26 with one exception: 02-290) for all samples, typical of detrital material mainly derived from the upper continental crust. Ce_N/Ce^* is in all quartz–arenites positive (>1) and close to 1 in the wackes, and slightly below 1 in mudrocks (0.91–0.96;

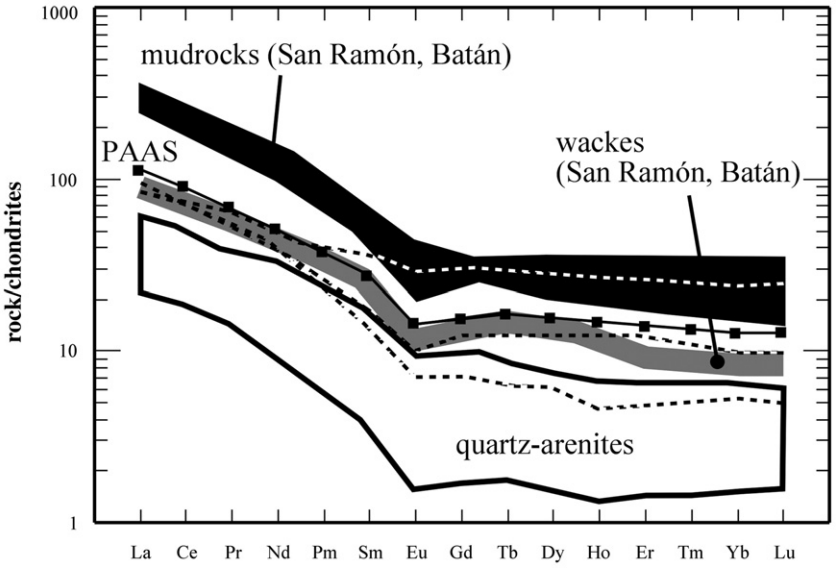

Fig. 6. Chondrite normalized samples of the Balcarce Formation (after Taylor and McLennan, 1985). Fine black line with squares represents PAAS (Post-Archaean Average Australian Shale after Nance and Taylor, 1976); black area = mudrocks; white area with black envelope = quartz–arenites; grey = wackes; stippled line = quartz–arenites (San Ramón, Batán).

Table 1 supplemental data). Eu_N/Eu^* is a parameter used to evaluate the abundance of plagioclase in an igneous rock or its sedimentary derivate (e.g. McLennan et al., 1990). Despite one sample (SD10), all quartz–arenites have values below 0.7, typical for UCC (after Taylor and McLennan (1985): 0.65). In contrast, the mudrocks show higher values (0.66 to 0.83) closer to 1 and point to the influence of an intermediate or mafic source.

5.5. Trace element provenance

Trace elements like Ti, Th, Sc and Zr and REE are particularly useful for provenance analysis as they are insoluble and usually immobile under surface conditions, thus preserving characteristics of the source rocks in the sedimentary record and robust provenance indicators (e.g. McLennan et al., 1990, 1993).

Th/Sc versus Zr/Sc ratios (Fig. 7) show a strong reworking component for the quartz–arenites (average 87; Table 1 supplemental data). Three mudrocks and one wacke display Th/Sc ratios above 1, while all other samples of these lithotypes have very low ratios (<0.5; Table 1 supplemental data). This is mainly a result of massive enrichment in Sc concentrations as Th and Zr content are comparable with typical UCC or higher. However, although the wackes have low Th/Sc ratios most of their Al_2O_3 is comparable to or lower than UCC (Table 1 supplemental data) and not related to the influence of kaolinite.

Trace element ratios such as La/Th, La/Sc, Zr/Sc, Ti/Zr and Th/Sc have been used successfully to discriminate tectonic settings (Bhatia and Crook, 1986; Floyd and Leveridge, 1987). Nonetheless, such approach must be used with caution since it has been shown that specific tectonic settings do not necessarily produce sedimentary rocks with unique geochemical signatures (McLennan et al., 1990; Bahlburg, 1998). Ti/Zr ratios versus La/Sc are shown in Table 1 supplemental data only. All quartz–arenites point to a rifted or passive margin setting, as their La/Sc ratios are high (>7; after Floyd and Leveridge (1987)) and Ti/Zr are relatively low (<12) expected for quartz-rich recycled clastic rocks. Wackes and mudrocks can be divided in two groups. One group displays an affinity to a typical UCC (La/Sc between 2 and 6; Ti/Zr<16). The second group is highly enriched in Ti and reflects an oceanic arc environment (after Floyd and

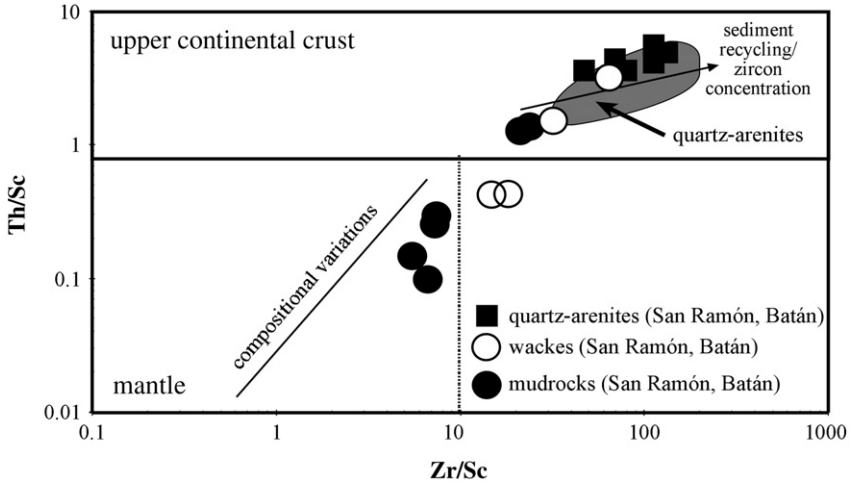

Fig. 7. Provenance plot after McLennan et al. (1990) showing clearly the compositional differences between the quartz–arenites, wackes and mudrocks.

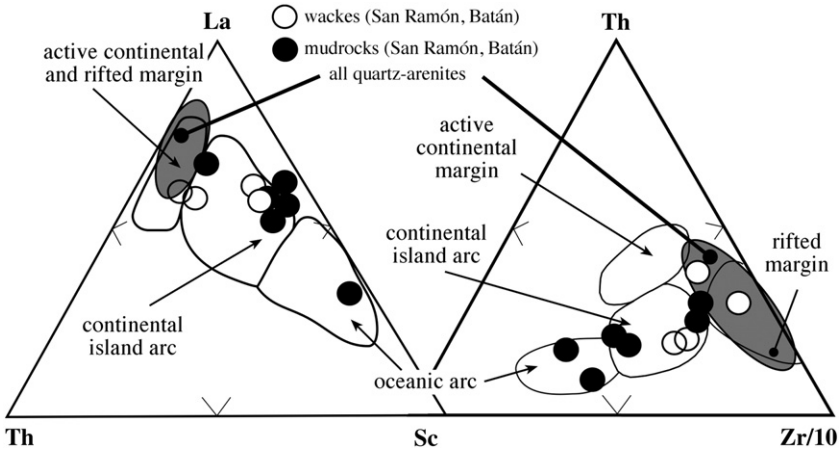

Fig. 8. Analysing the provenance by using relations of La, Sc, Th and Zr (after Bhatia and Crook, 1986). All quartz–arenites are grouped together as their compositions are nearly identical. The transitional character of the wackes caused by mixing of two different source components can be observed.

Leveridge (1987)). Nevertheless, these trends have to be interpreted carefully (see below).

In triangular relationships (Fig. 8) of La–Sc–Th–Zr, the quartz–arenites display a typical rifted margin composition, and the wackes and mudrocks follow a trend towards an oceanic environment. Although these lithotypes are strongly enriched in Zr (up to four times UCC; Table 1 supplemental data), some samples plot into an arc-related field because of high Sc concentrations, hence the influence of a mafic source.

6. Single grain chemistry

6.1. Tourmaline

Major element chemistry of tourmaline (12 representative data sets of 80 analysed grains; Table 3a) revealed that the grains represent schorl, based on their Si, Fe, Na, Al and Ti concentrations according to values from Deer et al. (1996) only Ca and Mg are slightly different.

Table 3
Chemical analyses of selected heavy minerals by microprobe measurements.

a)

Tourmaline		1	2	3	4	5	6	7	8	9	10	11	12	Schorl
FeO	%	12.56	13.33	14.16	12.30	12.10	12.31	12.30	12.03	12.29	11.89	11.84	12.34	15.11
MnO	%	0.47	0.24	0.07		0.16	0.22	0.24	0.05	0.02	0.23	0.31	0.14	0.25
TiO_2	%	0.69	0.67	0.58	0.38	0.33	0.36	0.61	0.50	0.45	0.54	0.59	0.47	0.41
CaO	%	0.11	0.07	0.17	0.01		0.05	0.14	0.07	0.08	0.08	0.22	0.07	0.21
Na_2O	%	2.08	2.06	2.31	1.86	1.86	1.84	1.85	1.77	1.85	1.90	1.88	1.78	1.92
SiO_2	%	35.21	35.95	36.17	37.38	37.52	37.59	38.23	39.88	38.34	38.65	38.94	39.22	33.78
Al_2O_3	%	32.75	33.68	34.00	34.24	34.47	33.88	33.76	33.54	33.58	34.29	34.24	34.12	33.80
MgO	%	1.71	1.74	1.64	1.93	2.06	1.98	1.90	1.83	1.99	2.06	1.96	1.99	0.74
Cr_2O_3	%		0.05	0.03		0.13	0.10	0.05	0.06		0.07		0.40	
K_2O	%	0.12	0.67		0.07	0.17	0.02		0.07	0.03			0.03	0.11
BO*	%	10.00	10.00	10.00	10.00	10.00	10.00	10.00	10.00	10.00	10.00	10.00	10.00	
Sum	%	95.69	98.46	99.11	98.17	98.79	98.34	99.07	99.79	98.62	99.71	99.98	100.56	86.33

b)

Rutile		1	2	3	4	5	6	7	8	9	10	11	12	13	14	15	16	17
Nb_2O_5	%	0.13	0.15	0.37	0.32	0.12	0.13	0.37	0.05	0.18	0.41	0.14	0.3	0.22	0.11	0.38	0.15	0.46
Cr_2O_3	%	0.3	0.22	0.17	0.22	0.03	0.15	0.05	0.12	0.22	0.14	0.25	0.14	0.09	0.03	0.08	0.22	0.15
Nb	ppm	937	1063	2552	2202	860	909	2587	322	1231	2832	944	2119	1524	797	2671	1056	3181
Cr	ppm	2039	1471	1156	1485	226	1013	356	835	1498	951	1731	978	602	178	541	1512	992

c)

Chromites		1	2	3	4	5	6	7	8	9	10	11	12	13	14	15
Al_2O_3	%	22.66	17.77	21.28	17.07	17.49	17.51	19.94	21.36	18.87	18.79	24.12	17.28	18.86	19.25	18.98
MgO	%	10.90	9.63	10.07	8.78	9.19	9.48	9.59	10.24	9.41	9.52	9.33	8.82	8.24	8.55	8.68
FeO	%	17.31	21.56	20.50	21.57	21.01	21.65	20.31	19.75	20.47	19.72	18.17	20.96	21.26	21.79	25.41
MnO	%	0.44	0.55	0.58	0.57	0.55	0.56	0.64	0.34	0.60	0.65	0.71	0.48	0.39	0.15	0.52
TiO_2	%	0.46	1.10	0.71	1.11	1.14	1.43	0.93	0.87	1.02	0.92	0.68	1.20	0.72	1.19	0.70
Cr_2O_3	%	46.16	48.00	45.42	48.85	48.84	47.13	46.56	45.73	48.68	49.37	45.66	46.42	48.66	47.74	45.14
CaO	%	0.11	0.00	0.43	0.11	0.10	0.11	0.04	0.02	0.10	0.07	0.11	0.06	0.00	0.00	0.00
Nb_2O_5	%	0.22	0.10	0.23	0.23	0.10	0.09	0.21	0.09	0.17	0.28	0.00	0.19	0.10	0.07	0.00
V_2O_5	%	0.20	0.53	0.54	0.32	0.57	0.37	0.34	0.45	0.41	0.63	0.26	0.38	0.61	0.41	0.43
Sum	%	98.46	99.24	99.77	98.62	98.98	98.33	98.57	98.85	99.73	99.96	99.03	95.79	98.85	99.16	99.86
Cr#		0.51	0.58	0.53	0.60	0.59	0.58	0.55	0.53	0.57	0.58	0.50	0.58	0.57	0.56	0.55
Fe^{3+}		0.03	0.70	0.03	0.07	0.07	0.08	0.05	0.05	0.08	0.04	0.03	0.08	0.03	0.08	0.04

a) Tourmaline chemistry, selected were 12 representative grains of 80 measurements. *Boron cannot be measured by microprobe and is calculated according to literature data from Deer et al. (1996). b) Rutile chemistry. c) Chromite chemistry. Cr# = Cr/(Cr + Al); Fe^{3+} calculated as discussed in the chapter "Sampling and analytical methods."

Low but variable concentrations in K (0.02 to 0.8%) and Mn (0.02 to 0.4%) were observed. Henry and Guidotti (1985) propose a classification scheme based on Al–Fe–Mg–Ca concentrations in tourmalines. The tourmalines from our study then derived from Li-poor granitoids and associated pegmatites and aplites (Fig. 9a).

6.2. Amphibole

The major element chemistry of the few analysed grains points to Fe–Mg-rich amphiboles, which are Na-free with only low concentrations in Mn, Ca and Cr (not shown here); hence, excluding high-grade metamorphic iron formations as source rocks (Deer et al., 1996). Comparable chemical results are given by Tiba et al. (1970) for anthophyllite and Haslam and Walker (1971) for cummingtonite, respectively. Cummingtonite can be found in intermediate rocks, low-Ca amphibolites in metamorphosed basic igneous rocks. Anthophyllite can occur with Mg-rich cummingtonite (here not determined) in metamorphosed ultrabasic rocks (Deer et al., 1996). Conclusively, the high Fe and Mg content points to a metabasic protolith.

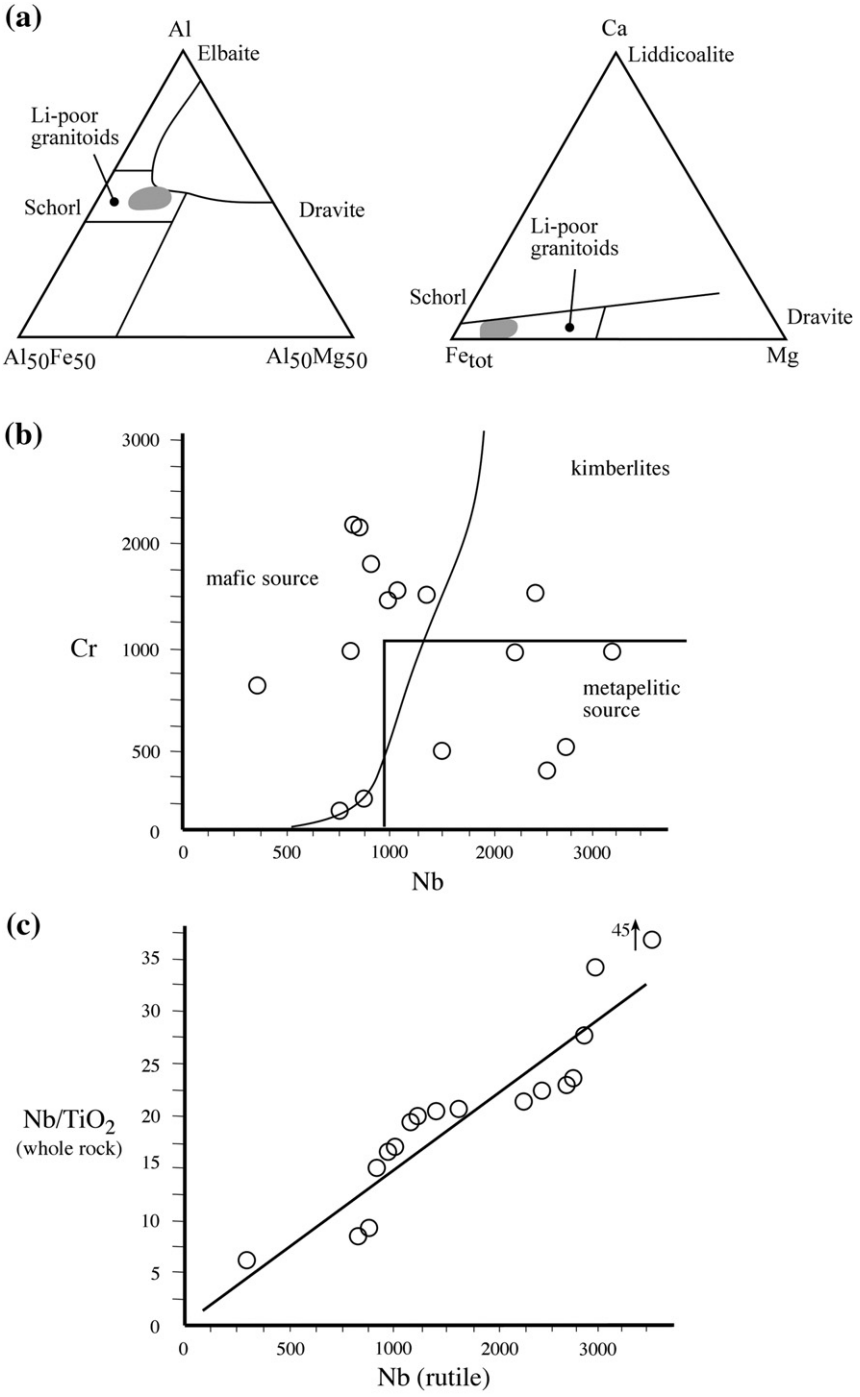

Fig. 9. a) Chemical discrimination of tourmaline based on their Al, Ca, Fe and Mg concentration (after Henry and Guidotti, 1985). The composition points to schorl derived from Li-poor granitoids and their apophyses. b) Cr and Nb concentrations in detrital rutile (after Zack et al., 2002) pointing to two different protoliths for the grains. c) Correlation between Nb in rutiles and Nb/TiO_2 ratios of the whole rock. If rutile is responsible for the whole-rock budget of Nb (and thus Ta and Ti) a positive correlation (straight black line) should be observable (after Zack et al., 2002), which is here not the case.

6.3. Rutile

Rutile can be divided in hydrothermal originated and detrital grains. Rutiles, which developed a rim alteration, were discarded for analyses. Trace element mobility is reported to be extremely rare in rutile (Zack et al., 2004). This was double-checked by spot analyses comparing centre with border for each grain. Cr and Nb concentrations were determined in detrital rutile and plotted against each other (Fig. 9b). Two fractions can be observed tentatively. One group of rutiles displays Nb concentration below 1500 ppm and the second group between 2000 to 3500 ppm (Table 3b). Both groups are variable in Cr (200 to 2000 ppm), but do not point to a kimberlitic source. Zack et al. (2002) defined different protoliths for rutiles (based on Cr–Nb concentrations), either derived from basaltic eclogites (low Nb and low Cr concentration), gabbroic eclogites (variable Nb and high Cr) and metapelites with higher Nb but rather low Cr concentrations. The authors show that in eclogites, the concentration of TiO_2, Nb, Ta, W and Sb is controlled by rutile if the ratios Nb/TiO_2 and Cr/TiO_2 of the whole rock correlate positively with Nb, and Cr concentrations in the rutile, respectively. However, in the present case study, the rocks are enriched with chromites; thus, the positive correlation of Cr to Cr/TiO_2 (whole rock) cannot be applied. Fig. 9c shows the correlation of Nb (in rutile) vs. Nb/TiO_2 (whole rock) and only a few rutiles are correlative exactly with the whole-rock composition. Although the variation is not large, other phases than detrital rutile might have had affected the Ti and Nb budget in the Balcarce Formation.

6.4. Chromite

Chrome spinel is a petrogenetic indicator for basic and ultramafic rocks, as it contains several cations whose atomic ratios vary according to physico-chemical conditions of the parent magma like cooling rate, crystallization temperature, composition, and oxygen fugacity (i.e. Evans and Frost, 1975; Dick and Bullen, 1984; Sack and Ghiorso, 1991; Arai, 1992). Chromites are widely used in the classification of origin and tectonic setting of mantle-derived peridotites (e.g. Dick and Bullen, 1984; Arai, 1992; Kamenetsky et al., 2001). Thus, detrital chromites can reveal important information about the source composition of sedimentary rocks (e.g. Oberhänsli et al., 1999; Asiedu et al., 2000; Zhu et al., 2004).

Fig. 10a demonstrates the variation of chromite compositions (Table 3c) and plot in a 90% confidence field for Cr-rich chromites (Barnes and Roeder, 2001). Metamorphic rims were not observed. Plotting TiO_2 against Al_2O_3 the chromites of the Balcarce Formation point as protoliths to either mid-ocean ridge basalts or arc basalts (Fig. 10b). The relatively high TiO_2 concentrations suggest a volcanic source (Kamenetsky et al., 2001). The TiO_2 concentrations of the grains vary only slightly as the Cr# [$Cr/(Cr+Al)$] is constant, thus in Fig. 10c the samples show a spread from the defined mid-ocean ridge basalt (MORB) field towards a combined field of MORB and island-arc basalts (after Arai, 1992). However, the low Fe^{3+} values (<0.1) point to a MORB (or back-arc MORB) related source rock (Fig. 10d; Arai, 1992). Nevertheless, the homogeneity of chromites from the Balcarce Formation is compelling, and their angular shape points to a geographically relatively closely related source.

7. Discussion

7.1. Geochemical constraints on provenance

The Balcarce Formation is composed of moderately to poorly sorted quartz–arenites, and kaolinite-rich wackes and mudrocks with pyroclastic components. Alteration of the wackes can be identified petrographically by the often complete replacement of feldspar by kaolinite. The relative depletion of feldspar in wackes and mudrocks might be related to extreme weathering conditions or a paucity of this mineral in the source rocks. A homogeneous rhyolitic to rhyo-dacitic composition for all quartz–arenites, and some wackes and mudrocks can be observed. Samples from the quarries San Ramón and Batán are partly enriched in Nb over Y and show a trend to an alkaline composition. This can be caused by the observed addition of hydrothermal rutile. However, rutile is not responsible for the entire Ti and Nb budget in the samples as shown above (Fig. 9c). Thus, a typical UCC source was mixed with another component, not existent in the quartz–arenites.

The quartz–arenites are enriched in Cr (Table 1 supplemental data), which is reflected in the abundance of angular chromite (Fig. 4h), while mudrocks and wackes are enriched in Zr, Hf and Sc. The strong enrichment of Zr in the mudrocks may be caused by a source component, neither visible or identified or never shed into the associated quartz–arenites. Differences between the mudrocks and the wackes in San Ramón and Batán are observable in higher concentrations of LILE in the former. This can be a product of the ability of clay minerals to incorporate easily larger ions in their crystal structure (e.g. McLennan et al., 1993). The high concentration of Sc found in both, mudrocks and wackes, does not correlate with other compatible elements or Al_2O_3 necessarily, which points to the influence of a rather intermediate source mixed with a fractionated felsic component to result in a typical UCC signature.

Recycled sediments and sedimentary rocks allow expected enrichment in Zr, reflecting zircon addition (e.g. McLennan et al., 1990; Zimmermann and Bahlburg, 2003), apart from chromite. The influence of chromite disappears in the wackes and mudrocks, and as the wackes and mudstones are rather immature sediments; sorting then was a subordinated factor. Therefore detritus from the chrome-delivering mafic source could not reach the latter rocks, even though chromite and zircon have a comparable specific density. This basic component is substituted by other sources, one enriched in Sc (intermediate), the other in Zr (Hf, Yb respectively), hence felsic, most probably sorted out of the quartz–arenitic detrital record. Besides chromite, other mafic minerals, such as strongly weathered pyroxene, amphibole, and rutile from mainly metabasaltic rocks are detected. Plagioclase is not preserved, either because the mafic component was devoid of it or the mineral was weathered.

REE patterns are relatively homogeneous throughout all three groups and show similar patterns as PAAS, either due to a result of mixing or to similar sources of typical UCC with few exceptions caused by heavy mineral addition (Fig. 6). Mudrocks and wackes display slightly lower negative Eu* anomalies (Table 1 supplemental data) and imply the addition of a less fractionated source, probably of andesitic origin. Strong enrichment of heavy REE (HREE) in the mudrocks can be explained by zircon addition. High Zr/Sc ratios are caused by very low Sc concentrations in the quartz–arenites, while some wackes and mudrocks show lower Th/Sc and Zr/Sc ratios but plot in the area of typical UCC (Fig. 7; Table 1 supplemental data). However, some samples display both low Th/Sc and Zr/Sc ratios, despite their high Zr concentrations (see Table 1 supplemental data). This points to the mixing of a closely related volcanic arc or mafic component with a typical UCC source. Often used Ti/Zr and La/Sc ratios show a similar tendency (not shown here; Table 1 supplemental data). While Ti enrichment may be influenced by hydrothermal processes, the large spread of La/Sc ratios clearly points to different source compositions, as quartz–arenites comprise high La/Sc ratios (>7) and only some wackes are between 4 and 7 (UCC after McLennan et al. (2006) = 2.2). If Ti is not used as a provenance indicator (Fig. 8) results are similar. As the less fractionated source becomes dominant (marked by high Sc concentrations), samples of the wackes and mudrocks point to an oceanic or continental arc. The detritus for the high concentrations in Zr and Sc must have been derived from a geographically closely related source, as the wackes and mudstones do not show sedimentological and geochemical characteristics of effective recycling.

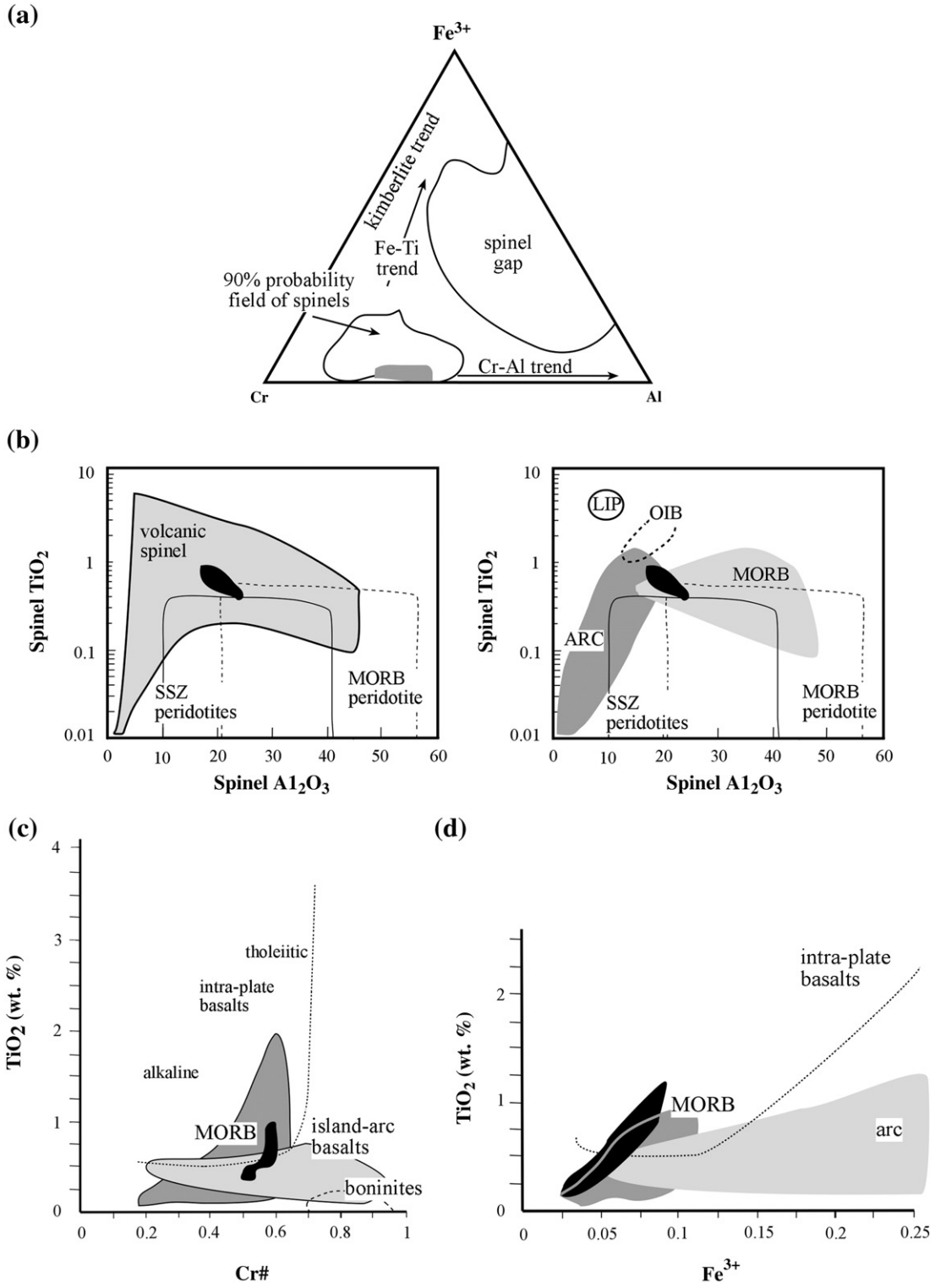

Fig. 10. Chemical composition of chromites to discriminate their protoliths. a) Fe^{3+}–Al–Cr relations in chromites (after Barnes and Roeder, 2001) show the chemical homogeneity of the separated grains (greyish field) with a typical Cr-rich composition plotting in the 90% probability field after Barnes and Roeder (2001). b) Left: Al_2O_3 vs. TiO_2 (after Kamenetsky et al., 2001) to demonstrate a volcanic origin for the chromite grains (black field); right: Al_2O_3 vs. TiO_2 (after Kamenetsky et al., 2001) used for the identification of the protolith. The chromites (black field) plot in an overlapping field of MOR basalts and basalts formed in volcanic arcs. Excluded are basalts formed in LIP and OI setting. LIP; large igneous provinces; OIB = oceanic island basalt; SSZ = supra subduction zone; MORB = mid-ocean ridge basalts. c) Cr# vs. TiO_2 are used to define the tectonic setting of the protoliths (after Arai, 1992). The chromite grains (black field) plot again in an overlapping field defined by island-arc basalts and MORB. d) Fe^{3+} vs. TiO_2 (after Arai, 1992) for the chromite grains (black field) would define a MORB derivation rather than an island arc. However, Fe^{3+} are calculated and not directly measured, thus they have to be interpreted with caution.

Chemical analyses of the heavy mineral fraction allowed a more detailed characterisation of the source components. Detrital tourmaline revealed a Li-poor granitic source, with associated aplites and pegmatites (Fig. 9a). Detrital rutile defines different sources: (i) mafic rocks and (ii) metapelites (Fig. 9b). Chromites are mostly angular and large (see Fig. 4h) and derived from a not metamorphic MORB source (Fig. 10c–d), hence, from a different mafic source area.

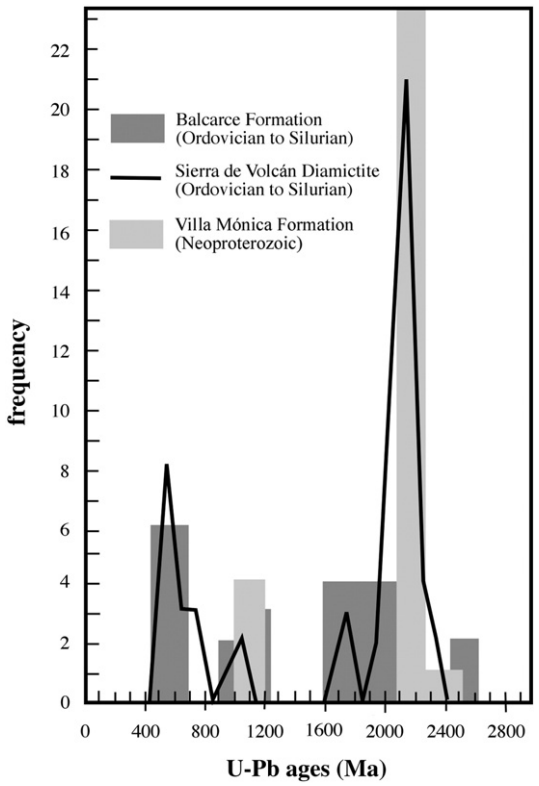

Fig. 11. Detrital zircon ages (in millions of years) of the Balcarce Formation (Ordovician–Silurian), Sierra de Volcán Diamictite (Hirnantian), and the Neoproterozoic Villa Monica Formation (data from Rapela et al., 2007; Van Staden et al., 2009).

7.2. Regional constraints on provenance

The felsic input into the Balcarce Formation was elucidated by detrital zircon dating (Rapela et al., 2007) and pointed to typical sources from the Río de la Plata craton, which coincides with results from the underlying or associated Sierra del Volcán Diamictite (Van Staden et al., 2009) and the Villa Mónica Formation (Rapela et al., 2007). Dominant detrital material from sources far to the north, Uruguay, might be discarded as zircons older than 2.6 Ga (Rapela et al., 2007) are only sparse, but those from Palaeoproterozoic and Neoproterozoic to Lower Paleozoic rocks in that area are abundant (Van Staden et al., 2009; Fig. 11).

Underlying clastic rocks of the Sierras Bayas Group (Fig. 2) are mainly composed of well-rounded quartz or very fine clastic material and carbonates and cannot be the main source of the Balcarce Formation (e.g. Poiré, 1987; Zimmermann et al., 2005). Only a few units of the Cerro Negro Formation comprise angular quartz (Poiré, 1987). Yet, the wackes and mudrocks of the Cerro Negro Formation must have been reworked strongly to form the quartz–arenites of the Balcarce Formation. However, the sediments of the Balcarce Formation are mostly coarser grained and relatively poorly sorted, comprising angular, sub-rounded and only a few well-rounded quartz grains. Simple normalization of REE (Fig. 12) to the underlying rocks shows that there are no direct relationships. Only the wackes of the Balcarce Formation show affinities in REE to some basement rocks and the Cerro Negro Formation (Fig. 12).

Felsic magmatic and metamorphic detritus mainly came from granitic intrusions of Cambrian and Ediacaran age (Rapela et al., 2007; Van Staden et al., 2009) and from Paleoproterozoic basement (Complejo Buenos Aires) of the Río de la Plata craton, added by from some few Mesoproterozoic grains of unknown provenance. The Complejo Buenos Aires (Fig. 2) also comprises metabasic rocks (Dalla Salda et al., 2006), which might be the precursor of the rutiles and amphiboles. However, not metamorphosed mafic rocks, which provided the chromites are not observed in the regional geology or were eroded away. Paleocurrent trends (Teruggi, 1964; Poiré et al., 2003) were assumed to be dominated by east west directed coast-parallel streams. Therefore, detrital provenance from areas in the east or west can be regarded, depending on the palaeogeography of the basin during the Cambrian and Ordovician (Rozendaal et al., 1999; Rapela et al., 2003). A source terrane for the chromites of the Balcarce Formation could have been obducted oceanic crust during the collision either oblique or orthogonal between the Precordillera Terrane and Gondwana. This could explain the input of MORB chromites with similar chemical composition into the Upper Ordovician Pavón Formation (Abre et al., in press), deposited on the Precordillera Terrane (Cingolani et al., 2003) on the other side of this hypothetical oceanic basin. Another explanation could be oceanic crust material developed from a Cambrian rift basin, which evolved from the upper Cambrian between the Kalahari Craton and the Río de la Plata craton (Rapela et al., 2003). However, this would imply a supply of chromite via oceanic upwelling.

The source of the volcanic input remains obscure as volcanic centres or lavas are not exposed in Lower Palaeozoic rocks in the eastern part of the Río de la Plata craton or on the Kalahari craton. During the Ordovician, volcanic arcs have been developed at the

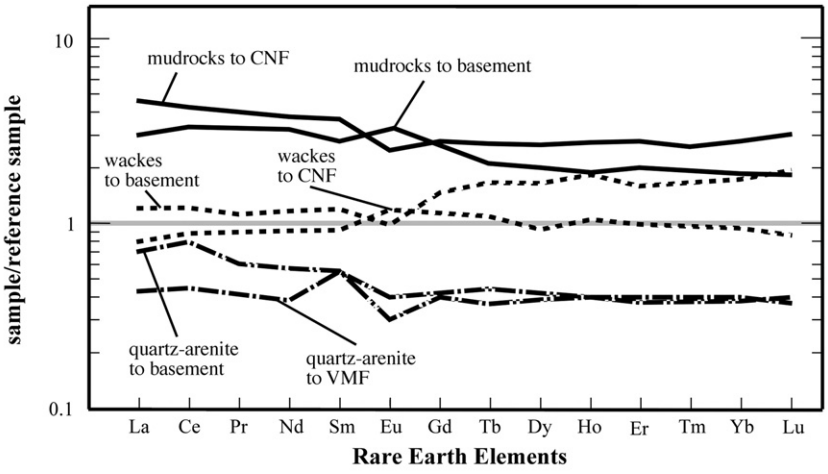

Fig. 12. Normalization of REE values of the different groups of the Balcarce Formation to selected underlying rock succession. Flat normalized or identical pattern are hardly to observe, only the wackes normalized to CNF is a good match; however, based on petrographical data the CNF is an unlikely source for the wackes of the Balcarce Formation (chondritic normalization of the REE after Taylor and McLennan (1985); CNF = Cerro Negro Formation; VMF = Villa Mónica Formation; stratigraphic position in Fig. 3; data for VMF and CNF unpublished).

border of Gondwana to the west of the Balcarce basin, such as the Puna–Famatina arc (Pankhurst et al., 1998; Zimmermann and Bahlburg, 2003), and far to the east, the Ross arc (Millar et al., 2002; Myrow et al., 2002; Federico et al., 2006). Most of the volcanic input is epiclastic and might have been introduced by an agent like wind in the absence of volcanic centres. Detrital volcanic zircons of similar ages are found in western South Africa at the base of the Emsian Gamka Formation of the Bokkeveld Group with paleocurrents from the west (Zimmermann et al., 2009). The cause of this volcanic input has not been studied yet, but it might be related to that of the Balcarce Formation, as both deposits are most likely similar in age (Van Staden et al., 2009; Fig. 13b).

7.3. Paleotectonic constraints on provenance

The main source for the detrital material for the Balcarce Formation was the exposed basement of the Río de la Plata craton and Lower Palaeozoic to Upper Neoproterozoic magmatic rocks. It seems that most areas of this craton were not covered by sedimentary successions of Neoproterozoic, in contrast to the thicker deposits in South Africa (Tankard et al., 1982). This implies rather small-scale basins, which developed prior to the Balcarce Formation, what does not allow them to be reliable to interpret crustal evolution of cratons, as they reflect most probably only the locally underlying rocks. This is obvious studying the contrast between the detrital zircon composition of the Balcarce Formation and the Neoproterozoic Villa Mónica Formation (Fig. 11), a highly reworked quartz-rich arenite (Zimmermann et al., 2005). The rather thin Neoproterozoic cover might as well explain, why these sources were not reworked in significant amounts into the Paleozoic basins (Fig. 12). The Neoproterozoic magmatic activity might be related to an active continental margin on the southern boundary of Gondwana (Cawood, 2005; Zimmermann et al., 2005, 2008) and/or to extensional tectonics (Rapela et al., 2003; Veevers, 2007). Hence, the felsic input, together with rutiles, is explainable by the regional geology. Detrital chromites derived from a non-metamorphic mafic source in close proximity, and the occurrence of volcanic debris, remains obscure.

The paleogeographic evolution of the areas towards the west of the Balcarce basin remains controversial (e.g. Thomas et al., 2004;

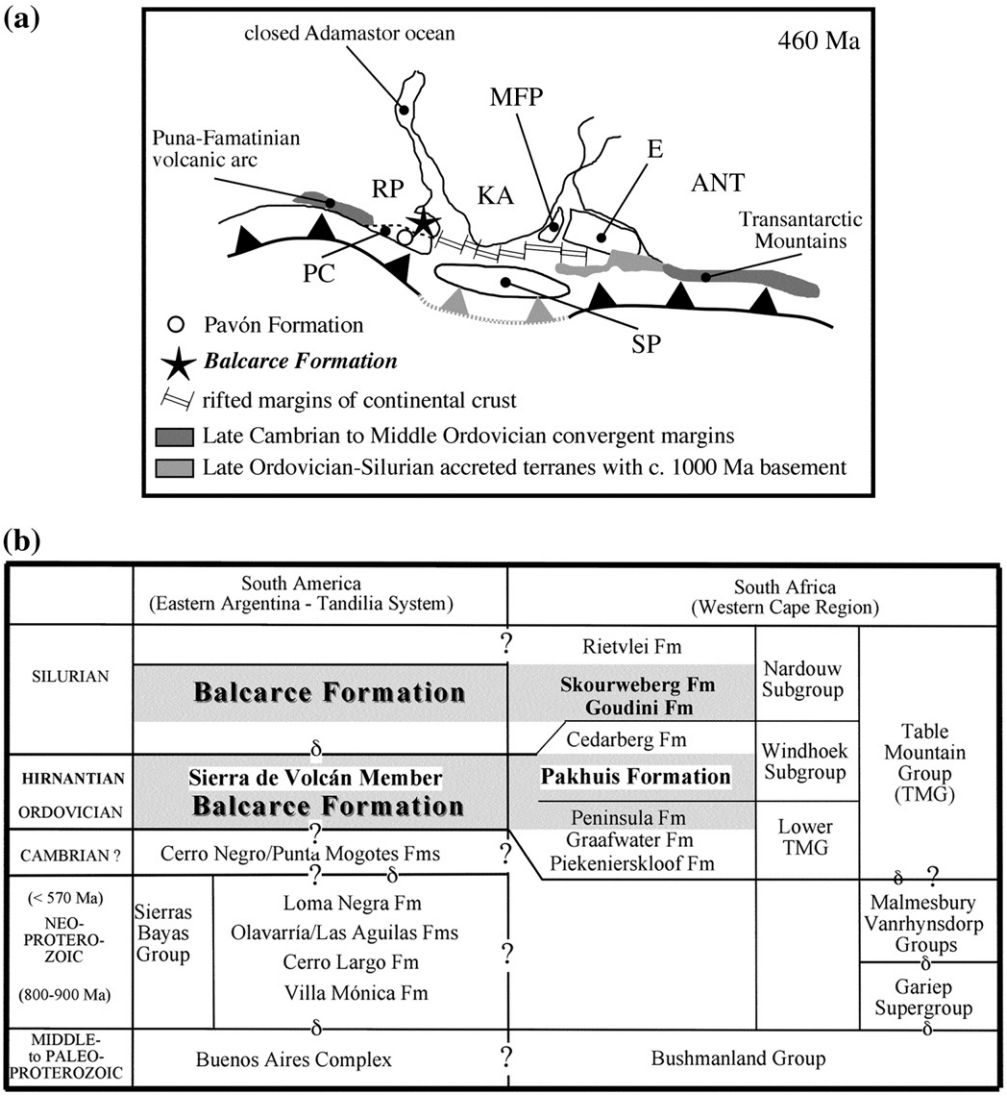

Fig. 13. a) Mid-Ordovician schematic paleogeographic and paleotectonic reconstruction of Western Gondwana (based on Cawood et al., 2001; Rapela et al., 2003, Zimmermann and Bahlburg, 2003; Pankhurst et al., 2006; Naidoo, 2008). The figure shows the location of the Balcarce Formation (black star), the rifted margins of continental crust and the inferred hypothetical active continental margin connecting Ordovician arc in Argentina and Antarctica. The stippled line between the Balcarce basin and the Pavón Formation marks a possible suture between the Precordillera and the Río de La Plata Craton. MFP: Malvinas/Falkland Plateau, SP: Southern Patagonia, PC: Precordillera Terrane, KA: Kalahari Craton, RP: Río de La Plata Craton, ANT = Antarctica; E = Ellsworth Mountains. b) Correlation and new lithostratigraphic table for the Tandilia System (revised after Van Staden et al., 2009) in comparison to age equivalent successions of South Africa (after De Beer et al., 2002). Grey areas mark successions proposed for correlation. In bold letters, the glacial diamictites deposited on the Río de la Plata and Kalahari cratons.

Gleason et al., 2007), hence, source areas are difficult to identify. However, a mafic complex could have existed towards the west, as the Upper Ordovician Pavón Formation, situated in central Argentina, received chemically similar chromite grains, most probably from eastern sources (Abre et al., in press). They might have come from an oceanic source situated between both outcrop regions (Fig. 13). The oceanic source has not to be necessarily a result of large-scale extension, but can also be related to back/retro-arc spreading or transtensional processes, which developed mafic crust. Extensional tectonic processes are also recorded from southern Africa along the modern border of the Kalahari craton during the Lower Palaeozoic (Le Roux, 1977; Tankard et al., 1982; Scheepers and Armstrong, 2002; Rapela et al., 2003) with the occurrence of small gabbroic bodies besides massive granitic intrusions (Scheepers and Armstrong, 2002). However, sedimentological explanations to shed chromites from oceanic ridges in an extensional tectonic regime onto coastal deposits, are complicated. Thus, the source of the chromites remains speculative and may only be resolved by means of age dating.

The input of magmatic zircons of Ordovician age into the Balcarce basin is perplexing. However, during early and middle Ordovician time a continental volcanic arc, the Famatina arc, was developed in what is now western Argentina (Pankhurst et al., 1998; Zimmermann and Bahlburg, 2003). We interpret that part of the pyroclastic contribution as derived from the Puna–Famatinian arc (Zimmermann and Bahlburg, 2003), which likely extended closer to the Balcarce depositional basin in central Argentina (Pankhurst et al., 2006). During the Ordovician, South America was oriented up side down and the active Ordovician arc was situated in the east. Wind direction on the southern hemisphere was oriented from east to west as the spinning of the earth deflected the wind in such a way as we proposed earlier (Zimmermann and Spalletti, 2005). However, the volcanic debris was reworked and might explain the time gap between the mainly Lower Ordovician Puna–Famatina arc and the deposition of the Balcarce Formation. Reported trace fossils do not pinpoint an exact age for the entire Balcarce Formation, as those of Silurian age occur only in the eastern part of the basin. Therefore we interpret for the Balcarce Formation an age range from Middle Ordovician to Lower Silurian. This would also fit better with the correlation made in Fig. 13b, where the Balcarce Formation is age equivalent with the Peninsula Formation, the Pakhuis Formation (glacial diamictite) and the base of the Nardouw Subgroup (Van Staden et al., 2009). Nonetheless, more data are needed to identify the exact age and genesis of the volcanic layers in both, the Balcarce and Cederberg Formations.

8. Conclusion

Detailed provenance studies on quartz–arenites of the Lower Paleozoic Balcarce Formation revealed a main derivation from upper crustal crystalline rocks of the Río de La Plata Craton into the Balcarce basin. Neoproterozoic sedimentary rocks can be excluded as main sources as trace element geochemistry and petrographic exclude a reworking of these successions. The wide age range of detrital zircons in the Balcarce Formation, in contrast to the Neoproterozoic rocks (Fig. 11), supports an interpretation that Neoproterozoic basins were rather small-scale and thus not representative of the regional crustal evolution of the Rio de la Plata craton. The detrital composition of the Balcarce Formation in contrast uncovers the input of various regional sources.

Petrography and whole-rock geochemistry and single grain chemistry revealed detrital material derived from old upper crustal source of magmatic, sedimentary, and subordinated felsic metamorphic (felsic and mafic) terranes. Major element analyses on chromites indicate a not exposed MORB protolith. However, source rock and mechanism to shed chromites from such sources into the Balcarce basin are unknown. The delivery of chromite may be associated with convergent tectonics causing the consumption and obduction of oceanic crust during pre-Upper Ordovician but post-tectonic times.

Trace element geochemistry of recycled pyroclastic material suggests volcanic arc sources. The provenance of the pyroclastic material may either be the Puna–Famatina arc, located in north and central Argentina, or a hypothetical active margin further to the south. These ash layers are equivalent in age to detrital volcanic zircons dated from Emsian sedimentary rocks of the Bokkeveld Group in western South Africa (Zimmermann et al., 2009).

The deposition of a glacial diamictite of Hirnantian age (Sierra del Volcán Diamictite) is interpreted as a member of the Balcarce Formation. Based on the stratigraphic re-location of the glacial diamictite and trace fossils, the Balcarce Formation is considered here to be Ordovician to Silurian in age. The Balcarce Formation can be correlated with similar rocks in South Africa, the Peninsula Formation, and the upper Table Mountain Group (Windhoek and Nardouw Subgroups), including the Hirnantian glacial deposit of the Pakhuis Formation.

The study demonstrates that simple provenance studies on quartz-rich sandstones can reveal important information for understanding Paleozoic basin evolution.

Acknowledgements

The financial support of the Department of Petroleum Engineering (UiS) made this publication finally possible. Daniel Poire is thanked for inspiring discussions during fieldwork. Analytical work was partly performed at the Central Analytical facility (SPECTRAU) of the University of Johannesburg, the former institution where UZ was employed. We would like to thank Gert Jan Weltje and James D. Gleason for the very helpful and inspiring reviews.

Appendix A. Supplementary data

Supplementary data associated with this article can be found, in the online version, at doi:10.1016/j.sedgeo.2009.02.002.

Appendix B. Sampling and analytical methods

Sampling

Samples were taken from the whole area of exposure of the Balcarce Formation (Fig. 1). Two outcrops, the quarries San Ramón and Batán (Fig. 1), were intensively sampled to characterise from the geochemical viewpoint the different facies types.

Petrography

Polished thin sections were prepared of representative samples for framework, matrix and cement mineral analyses with a light microscope and SEM.

Heavy mineral studies

Samples were crushed, sieved and cleaned in fractions each between 80 and 400 μm. This pre-concentrate was treated with bromoform ($\delta = 2.89\ g \cdot cm^{-3}$) to obtain the complete heavy minerals fraction, followed by an electromagnetic separation with a Frantz Isodynamic Separator to obtain a fraction enriched in chromites. Each of the fractions was embedded randomly into epoxy resin, avoiding a preference for a certain population, polished down and carbon coated.

Scanning electron microscope analysis (SEM)

The identification and characterisation (shape, size, fractures, inclusions, etc.) of the heavy minerals were done using scanning and back-scattered electron microscope using energy dispersive spectrometry (SEM-BSE-EDS). A JEOL JSM-5600 was used with a tungsten

filament and EDS analyses were carried out with a Noran X-ray detector and Noran Vantage software. The SEM-BSE-EDS system was set at 15 keV, a working distance of 20 mm and a live time of 60 s per spot.

Electron microprobe

Quantitative analyses of tourmaline, amphibole, rutile and chromite were carried out on a Cameca 355 electron microprobe with Oxford link integrated WDS/EDS, set at a voltage of 15 keV. Beam current diameter is between 2 and 5 μm; ZAF corrections were done according to standard procedures. Total iron measurements on chromites were calculated through a Visual Basic macro in Microsoft Excel based on the stoichiometric formula of spinels, in order to define Fe^{2+} and Fe^{3+}. Several authors (e.g. Wood and Virgo, 1989) pointed out that accuracy and precision of such calculations are not perfect, but precise and accurate enough to obtain Fe^{3+} and Fe^{2+} concentrations. Each grain was measured several times (five to eight spots in the centre) depending on grain size, and averages are reported in Table 1 supplemental data. Differences in major element composition from the rim to the core could not be observed and were tested for every grain.

X-ray diffraction (XRD)

Sample powders were mounted on a Philips X'Pert Pro. CoK_α X-rays were generated at 30 mA and 40 kV. The following scan parameters were used: angle range: 5° to 70° 2θ; scan speed: 3 s per degree. To obtain more accurate results for more complex samples the instrumental settings were changed to a scan speed of 18 s/degree and 0.02° step size.

ICP-MS analysis

Samples were cleaned for geochemical analyses. Weathered coats and veined surfaces were cut off. The rocks were crushed and milled in a Cr-steel dish to a very fine powder. The contamination of Cr never exceeds 150 ppm, as permanent monitoring of analytical results over years on soft and extreme hard rocks revealed, controlled by an internal standard. Absolute Cr values cannot be used for any calculations (Tables 2 and 1 supplemental data). Therefore, Cr values are only shown (Fig. 5b) to demonstrate trends. Major and trace element analyses were carried out by ICP-MS at ACME Laboratories (Vancouver, Canada).

References

Abre, P., Cingolani, C., Zimmermann, U., Cairncross, B., in press. Detrital chromian spinels from Upper Ordovician deposits in the Precordillera terrane, Argentina: a mafic crust input. Journal of South American Earth Sciences. doi:10.1016/j.jsames.2009.04.005.

Amstrong-Altrin, J.S., Verma, P.S., 2005. Critical evaluation of six tectonic setting discrimination diagrams using geochemical data of Neogene sediments from known tectonic settings. Sedimentary Geology 117, 115–129.

Arai, S., 1992. Chemistry of chromian spinel in volcanic rocks as a potential guide to magma chemistry. Mineralogical Magazine 56, 173–184.

Asiedu, D.K., Suzuki, S., Shibata, T., 2000. Provenance of sandstones from the Lower Cretaceous Sasayama Group, inner zone of southwest Japan. Sedimentary Geology 131, 9–24.

Bahlburg, H., 1998. The geochemistry and provenance of Ordovician turbidites in the Argentinian Puna. In: Pankhurst, R.J., Rapela, C.W. (Eds.), The Proto-Andean Margin of Gondwana. Geological Society London Special Publication, vol. 142, pp. 127–142.

Barnes, S.J., Roeder, P.L., 2001. The range of spinel compositions in terrestrial mafic and ultramafic rocks. Journal of Petrology 42, 2279–2302.

Bhatia, M.R., Crook, K.A.W., 1986. Trace elements characteristics of graywackes and tectonic setting discrimination of sedimentary basins. Contributions to Mineralogy and Petrology 92, 181–193.

Boles, J.R., Franks, S.G., 1979. Clay diagenesis in Wilcox Sandstones of Southwest Texas: implications of smectite diagenesis on sandstone cementation. Journal of Sedimentary Petrology 49, 55–70.

Cawood, P.A., 2005. Terra Australis Orogen: Rodinia breakup and development of the Pacific and Iapetus margins of Gondwana during the Neoproterozoic and Paleozoic. Earth-Science Reviews 69, 249–279.

Cawood, P.A., McCausland, P.J.A., Dunning, G.R., 2001. Opening Iapetus: constraints from the Laurentian margin in Newfoundland. Geological Society of America Bulletin 113, 443–453.

Cingolani, C., Manassero, M., Abre, P., 2003. Composition, provenance and tectonic setting of Ordovician siliciclastic rocks in the San Rafael Block: southern extension of the Precordillera crustal fragment, Argentina. Journal of South American Earth Sciences, Special Issue on the Pacific Gondwana Margin (IGCP 436) 16 (1), 91–106.

Dalla Salda, L., Spalletti, L., Poiré, D.G., De Barrio, R., Echeveste, H., Benialgo, A., 2006. Tandilia. In: Aceñolaza, F.G. (Ed.), Temas de la Geología Argentina I; INSUGEO. Serie Correlación Geológica, vol. 21, pp. 17–46.

De Beer, Gresse, P.G., Theron, J.N., Almond, J.E., 2002. The Geology of the Calvinia Area; Council for Geoscience, Sheet 3118 Calvinia, 92p.

Deer, W.A., Howie, R.A., Zussman, J., 1996. The Rock Forming Minerals, 2nd Edition. Longman, London, pp. 1–696.

Dick, J.B., Bullen, T., 1984. Chromian spinel as a petrogenetic indicator in abyssal and alpine-type peridotites and spatially associated lavas. Contributions to Mineralogy and Petrology 86, 54–76.

Dristas, J.A., Frisicale, M.C., 1987. Rocas piroclasticas en el sector suroeste de las Sierras Septentrionales de la Provincía de Buenos Aires. Revista de la Asociación Argentina de Mineralogía, Petrología y Sedimentología 18, 33–45.

Dristas, J.A., Frisicale, M.C., 1996. Geochemistry of an altered pyroclastic suite interbedded in the sedimentary cover of the Tandilia Area, Buenos Aires Province, Argentina. Zentralblatt für Geologie und Paläontologie, Teil I 7/8, 659–675.

Evans, B.W., Frost, B.R., 1975. Chrome-spinel in progressive metamorphism—a preliminary analysis. Geochimica et Cosmochimica Acta 39, 959–972.

Federico, L., Giovanni Capponi, G., Laura Crispini, L., 2006. The Ross orogeny of the transantarctic mountains: a northern Victoria Land perspective. International Journal of Earth Sciences 95, 759–770.

Fedo, C.M., Nesbitt, H.W., Young, G.M., 1995. Unravelling the effects of potassium metasomatism in sedimentary rocks and paleosoils, with implications for paleoweathering conditions and provenance. Geology 23, 921–924.

Floyd, P.A., Leveridge, B.E., 1987. Tectonic environment of the Devonian Gramscatho basin, south Cornwell: framework mode and geochemical evidence from turbidite sandstones. Journal of the Geological Society London 144, 531–542.

Floyd, P.A., Keele, B.E., Leveridge, B.E., Franke, W., Shail, R., Dörr, W., 1990. Provenance and depositional environment of Rhenohercynian synorogenic greywackes from the Giessen Nappe, Germany; Geologische Rundschau 79, 611–626.

Fralick, P., 2003. Geochemistry of clastic sedimentary rocks: ratio techniques. In: Lentz, D.R. (Ed.), Geochemistry of Sediments and Sedimentary Rocks: Evolutionary Considerations to Mineral-Deposit-Forming Environments. Geological Association of Canada, GEOText, vol. 4, pp. 85–104.

Gleason, J.D., Finney, S.C., Peralta, S.H., Gehrels, G.E., Marsaglia, K.M., 2007. Zircon and whole-rock Nd–Pb isotopic provenance of Middle and Upper Ordovician siliciclastic rocks, Argentine Precordillera. Sedimentology 54, 107–136.

Haslam, H.W., Walker, D.G., 1971. A metamorphosed pyroxenite at Nero Hill, central Tanzania. Mineralogical Magazine 38, 58–63.

Henry, D.J., Guidotti, C.V., 1985. Tourmaline as a petrogenetic indicator mineral: an example from the staurolite-grade metapelites of NW Maine. American Mineralogist 70, 1–15.

Hurowitz, J.A., McLennan, S.M., 2005. Geochemistry of Cambro-Ordovician sedimentary rocks of the Northeastern United States: changes in sediment sources at the Onset of Taconian Orogenesis. Journal of Geology 113, 571–587.

Iñiguez Rodríguez, A.M., 1999. La cobertura sedimentaria de Tandilia. In: Caminos, R. (Ed.), Geología Argentina. Subsecretaría de Minería de la Nación Servicio Geológico Minero Argentino Instituto de Geología y Recursos Minerales, vol. 29, pp. 101–106.

Kamenetsky, V.S., Crawford, A.J., Meffre, S., 2001. Factors controlling chemistry of magmatic spinel: an empirical study of associated olivine, Cr-spinel and melt inclusions from primitive rocks. Journal of Petrology 42, 655–671.

Le Roux, J.P., 1977. The Stratigraphy, Sedimentology and Structure of the Cango Group North of Oudtshoorn, C.P. M.Sc. Thesis (unpublished), University of Stellenbosch. 149pp.

McLennan, S.M., Taylor, S.R., McCulloch, M.T., Maynard, J.B., 1990. Geochemical and Nd–Sr isotopic composition of deep-sea turbidites: crustal evolution and plate tectonic associations. Geochimica et Cosmochimica Acta 54, 2015–2050.

McLennan, S.M., Hemming, S., McDaniel, D.K., Hanson, G.N., 1993. Geochemical approaches to sedimentation, provenance and tectonics. In: Johnsson, M.J., Basu, A. (Eds.), Processes Controlling the Composition of Clastic Sediments. Geological Society of America, Special Publication, vol. 284, pp. 21–40.

McLennan, S.M., Taylor, S.R., Hemming, S.R., 2006. Composition, differentiation, and evolution of continental crust: constrains from sedimentary rocks and heat flow. In: Brown, M., Rushmer, T. (Eds.), Evolution and Differentiation of the Continental Crust, pp. 92–134.

Millar, I.L., Pankhurst, R.J., Fanning, C.M., 2002. Basement chronology of the Antarctic Peninsula: recurrent magmatism and anatexis in the Palaeozoic Gondwana Margin. Journal of the Geological Society, London 159, 145–157.

Myrow, P.M., Pope, M.C., Goodge, J.W., Fischer, W., Palmer, A.R., 2002. Depositional history of pre-Devonian strata and timing of Ross orogenic tectonism in the central Transantarctic Mountains, Antarctica. Geological Society of America Bulletin 114, 1070–1088.

Naidoo, T. 2008. Provenance of the Neoproterozoic to Early Palaeozoic Kango Inlier, Oudtshoorn, South Africa. University of Johannesburg, unpublished MSc Thesis; 218pp.

Nance, W.B., Taylor, S.R., 1976. Rare earth element patterns and crustal evolution—I. Australian Post-Archean sedimentary rocks. Geochimica et Cosmochimica Acta 40, 1539–1551.

Nesbitt, H.W., Young, Y.M., 1982. Early Proterozoic climates and plate motions inferred from major element chemistry of lutites. Nature 299, 715–717.

Nesbitt, H.W., Young, G.M., McLennan, S.M., Keays, R.R., 1996. Effects of chemical weathering and sorting on the petrogenesis of siliciclastic sediments, with implications for provenance studies. Journal of Geology 104, 525–542.

Oberhänsli, R., Wendt, A.S., Goffé, B., Michard, A., 1999. Detrital chromites in metasediments of the East-Arabian continental margin in the Saih Hatat area: constraints for the Paleogeographic setting of the Hawasina and Semail basins (Oman Mountains). International Journal of Earth Sciences 88, 13–25.

Pankhurst, R.J., Rapela, C.W., Saavedra, J., Baldo, E., Dahlquist, J., Pascua, I., Fanning, C.M., 1998. The Famatinian magmatic arc in the central Sierras Pampeanas: an Early to Mid Ordovician continental arc on the Gondwana margin. In: Pankhurst, R.J., Rapela, C.W. (Eds.), The Proto-Andean Margin of Gondwana. Geological Society of London Special Publication, vol. 142, pp. 181–217.

Pankhurst, R.J., Ramos, A., Linares, E., 2003. Antiquity of the Río de la Plata craton in Tandilia, southern Buenos Aires province, Argentina. Journal of South American Earth Sciences 16, 5–13.

Pankhurst, R.J., Rapela, C.W., Fanning, C.M., Márquez, M., 2006. Gondwanide continental collision and the origin of Patagonia. Earth-Science Reviews 76, 235–257.

Poiré, D.G. 1987. Mineralogía y sedimentología de la Formación Sierras Bayas en el núcleo septentrional de las sierras homónimas, Partido de Olavarría, Provincia de Buenos Aires. PhD Thesis, Universidad Nacional de La Plata, Argentina.

Poiré, D.G., Spalletti, L.A., Del Valle, A., 2003. The Cambrian–Ordovician siliciclastic platform of the Balcarce Formation (Tandilia System, Argentina): facies, trace fossils, paleoenvironments and sequence stratigraphy. Geologica Acta 1, 41–60.

Rapela, C.W., Pankhurst, R.J., Fanning, C.M., Grecco, L.E., 2003. Basement evolution of the Sierra del la Ventana Fold Belt: new evidence for Cambrian continental rifting along the southern margin of Gondwana. Journal of the Geological Society, London 160, 613–628.

Rapela, C.W., Pankhurst, R.J., Casquet, C., Fanning, C.M., Baldo, E.G., González-Casado, J. M., Galindo, J., Dahlquist, J., 2007. The Río de la Plata craton and the assembly of SW Gondwana. Earth-Science Reviews 83, 49–82.

Rozendaal, A., Scheepers, R., Gresse, P.G., Le Roux, J.P., 1999. Neoproterozoic to Early Cambrian crustal evolution of the Pan-African Saldania Belts, South Africa. South African Journal of Geology 100, 1–10.

Sack, R.O., Ghiorso, M.S., 1991. Chromian spinels as petrogenetic indicators: thermodynamics and petrological applications. American Mineralogist 76, 827–847.

Scheepers, R., Armstrong, R., 2002. New U–Pb SHRIMP zircon ages of the Cape Granite Suite: implications for the magmatic evolution of the Saldania Belt. South African Journal of Geology 105, 241–256.

Schneider, N., 1993. Das lumineszenzaktive Strukturinventar von Quarzphänokristen in Rhyolithen. Göttinger Arbeiten zur Geologie und Paläontologie 60, 1–81.

Seilacher, A., Congolani, C., Varela, R., 2003. Ichnostratigraphic correlation of Early Palaeozoic sandstones in North Africa and Central Argentina. In: Salem, M.J., Oun, K.M. (Eds.), The Geology of Northwest Libya, pp. 275–292.

Tankard, A.J., Jackson, M.P., Erikson, K.A., Holiday, D.K., Hunter, D.R., Minter, W.E.L., 1982. Crustal Evolution of Southern Africa. Springer-Verlag, New York. 523 pp.

Taylor, S.R., McLennan, S.M., 1985. The Continental Crust: Its Composition and Evolution. Blackwell Scientific, Oxford. 312 pp.

Teruggi, M.E., 1964. Paleocorrientes y paleogeografía de las ortocuarcitas de la Serie de la Tinta (Provincia de Buenos Aires). Anales de la Comisión de Investigaciones Científicas de la Provincia de Buenos Aires V, 1–27.

Thomas, W.A., Astini, R.A., Mueller, P.A., Gehrels, G.E., Wooden, J.L., 2004. Transfer of the Argentine Precordillera terrane from Laurentia: constraints from detrital-zircon geochronology. Geology 32, 965–968.

Tiba, T., Hashimoto, M., Kato, A., 1970. An anthophyllite–hornblende pair from Japan. Lithos 3, 335–340.

Van Staden, A., Naidoo, T., Zimmermann, U., Germs, G.J.B., 2006. Provenance analysis of selected clastic rocks in Neoproterozoic to lower Paleozoic successions of southern Africa from the Gariep Belt and the Kango Inlier. South African Journal of Geology 109, 215–232.

Van Staden, A., Zimmermann, U., Gutzmer, J., Chemale Jr., F., Germs, G.J.B., 2009. Age of a Hirnantian glacial diamictite in eastern Argentina and consequences for the correlation with Lower Palaeozoic rocks in South Africa. Annual Meeting of the Norwegian Geological Society Vinterkonferansen 2009, Bergen, 13–15.1. 2009. Abstracts.

Veevers, J.J., 2007. Pan-Gondwanaland post-collisional extension marked by 650–500 Ma alkaline rocks and carbonatites and related detrital zircons: a review. Earth-Science Reviews 83, 1–47.

Winchester, J.A., Floyd, P.A., 1977. Geochemical discrimination of different magma series and their differentiation products using immobile elements. Chemical Geology 20, 325–343.

Wood, B.J., Virgo, D., 1989. Upper mantle oxidation state: ferric iron contents of lherzolite spinels by ^{57}Fe Mössbauer spectroscopy and resultant oxygen fugacities. Geochimica et Cosmochimica Acta 53, 1277–1291.

Zack, T., Kronz, A., Foley, S.F., Rivers, T., 2002. Trace element abundances in rutiles from eclogites and associated garnet mica schists. Chemical Geology 184, 97–122.

Zack, T., von Eynatten, H., Kronz, A., 2004. Rutile geochemistry and its potential use in quantitative provenance studies. Sedimentary Geology 171, 37–58.

Zhu, B., Kidd, S.F., Rowley, D.B., Currie, B.S., 2004. Chemical compositions and tectonic significance of chrome-rich spinels in the Tianba Flysch, Southern Tibet. Journal of Geology 112, 417–434.

Zimmermann, U., Bahlburg, H., 2003. Provenance analysis and tectonic setting of the Ordovician clastic deposits in the southern Puna Basin, NW Argentina. Sedimentology 50, 1079–1104.

Zimmermann, U., Spalletti, L.A., 2005. The provenance of the lower Palaeozoic Balcarce Formation (Tandilia System, Buenos Aires Province, Argentina). XVI Congreso Geológico Argentina, La Plata, 20.-23.9. 2005. Actas, vol. 3, pp. 203–210.

Zimmermann, U., Poiré, D.G., Gómez Peral, L., 2005. Provenance studies on Neoproterozoic successions of the Tandilia System (Buenos Aires province, Argentina)—preliminary data. XVI Congreso Geológico Argentino 4, 238–243.

Zimmermann, U., Tait, J.A., Miyazaki, T., Naidoo, T., 2008. Probable Neoproterozoic retro-arc basins on the southern Kalahari craton: the search for an active margin bordering southern Gondwana. 33th International Geological Congress Oslo, 6.-12.8. 2008. Abstract volume.

Zimmermann, U., Fourie, P., Naidoo, T., Chemale Jr., Nakamura, E., Kobyashi, K., Kosler, J., Beukes, N., Tait., J., 2009. Unroofing the Kalahari craton: Provenance data from Neoproterozoic to Paleozoic successions. Goldschmidt 2009. Abstract volume, Geochimica et Cosmochimica Acta.